Portland State University

PDXScholar

Dissertations and Theses

Dissertations and Theses

Spring 6-5-2019

Photoelectrochemical Catalysis of Hydrogen Peroxide with Tellurium Containing Chromophores

James Eliott Lohman
Portland State University

Follow this and additional works at: https://pdxscholar.library.pdx.edu/open_access_etds

 Part of the Chemistry Commons

Let us know how access to this document benefits you.

Recommended Citation

Lohman, James Eliott, "Photoelectrochemical Catalysis of Hydrogen Peroxide with Tellurium Containing Chromophores" (2019). *Dissertations and Theses.* Paper 5307.
https://doi.org/10.15760/etd.7180

This Thesis is brought to you for free and open access. It has been accepted for inclusion in Dissertations and Theses by an authorized administrator of PDXScholar. Please contact us if we can make this document more accessible: pdxscholar@pdx.edu.

Photoelectrochemical Catalysis of Hydrogen Peroxide with Tellurium Containing Chromophores

by

James Eliott Lohman

A thesis submitted in partial fulfillment of the
requirements for the degree of

Master of Science
in
Chemistry

Thesis Committee:
Theresa McCormick, Chair
Andrea Goforth
Jack Barbera

Portland State University
2019

© 2019 James Eliott Lohman

Abstract

Growing concerns over climate change and demand for energy world-wide have made development and implementation of alternative energy sources more necessary than ever. Many of the leading energy alternatives suffer from inconsistent energy production due to fluctuations in availability of natural resources, and the current methods of addressing the issue have tremendous ecological and social ramifications of their own. While fuels like hydrogen gas are providing some promise of relief, the scope of infrastructure changes necessary for implementation and the implicit hazards of the use of such fuels complicate their application as an immediate solution. However, hydrogen peroxide carries far fewer direct hazards than hydrogen gas, while producing comparable output. Additionally, since it exists as a liquid at room temperature and atmospheric pressure its potential application with existing infrastructure is far more attainable. While already in use in certain rocket technologies, peroxide fuel cells are still periphery energy production technology mainly due to the relatively high cost of producing hydrogen peroxide. In order for peroxide fuel cells to enter the mainstream and fulfill their potential as an alternative energy source, better and more efficient catalytic methods must be found for synthesis of hydrogen peroxide.

A class of chromophores known as tellurorhodamines have shown promise of providing an alternative approach to production of hydrogen peroxide. Specifically, 3,6-diamino-9-mesityl-telluroxanthylium, in a class of chromophores known as tellurorhodamines, has been shown to produce hydrogen peroxide by photocatalysis. This work describes the combination of properties that make

tellurorhodamines viable for photochemical catalytic production of hydrogen peroxide as well as *in-operando* production of a working current via electrochemical reduction of the catalyst within the same system, effectively creating a photoelectrochemical cathode. The amalgamation of photocatalytic and electrochemical methods in the simultaneous production and storage of energy is extremely desirable, though unprecedented, in the field of alternative energy. In that way, tellurorhodamnies present a unique opportunity among existing photoelectrochemical systems, which if applied could represent a new approach to addressing the looming energy crisis.

Acknowledgements

Though I lack any palpable grace in expressing the deep gratitude I feel for those who have helped me in my pursuit of higher education [and hopefully will continue to do so], I do feel the need to express that gratitude, clumsy as it may be. First and foremost, to my advisor, Dr.Theresa McCormick, for her guidance and infinite patience with my heel-dragging, especially considering that the course of this Master's thesis has been anything but conventional. Of course, to the rest of my thesis committee, Dr.Andrea Goforth and Dr.Jack Barbera, for their flexibility, insight, and understanding in this process. To my labmates for their support; especially Luke Lutkus and Irving Rettig, both of who had tangent projects which informed and supported my own.

To my undergraduate instructor, Dr.Thomas Betts, whose instruction was fundamental in my connection to the greater field of chemistry, and without whose encouragement I likely would not have pursued higher education. To my high school instructor, Mrs.Wallburga Weber, who will never read this, but had an immense impact on the course of my life, being the first to sincerely introduce me to the world of the physical sciences. To my family, without whom life in general, throughout the whole of my academic career, would have been considerably more unbearable.

To all of you, from the bottom of my heart: Thank you.

Table of Contents

List of Figures

List of Schemes

1. Tellurorhodamines to Produce Hydrogen Peroxide as Fuel

1.1 Introduction

Global energy consumption is a figure that can be broadly correlated to the progression and continued expansion of human civilization, and so consequently energy demand *should* only ever increase as years continue to pass. The controversy surrounding fossil fuels, and the destructive effect on ecology associated with their use, has made it clear that more research into affordable, clean, and diverse energy sources is necessary to sustain the continued evolution of our global society. Wind and solar technologies are the most widely recognized sources of renewable energy. The lack of an effective means of energy storage severely limits the feasible range of applications of renewable energies, especially solar and wind sources, which may be responsible for keeping renewables under the 10% of global consumption.[1]

Current energy storage methods are insufficient to provide a badly needed solution to the inconsistent availability of the sunlight across the Earth's surface over time. One could contend that the lack of storage options is the final blockade to eliminating the global community's reliance on fossil fuels. Even the most efficient batteries, being bulky and expensive in terms of the power they deliver, lack the qualities required to make them practical for implementation in the energy grid; that is not even to mention the ecological and social consequences associated with the manufacturing and refinement of batteries' composite materials.[1–3] Regardless of architecture, battery-structures cannot compete with small-molecule

motifs in terms of efficient energy storage on a global scale and while materials such as hydrogen gas have provided some promise, they are plagued by certain practical limitations imposed by existing infrastructure.[2,4,5] Those hardships are precisely why our society is still reliant on fossil fuels despite technological advancements and legislative incentivization for alternative energy sources. The research described herein will be aimed at addressing the storage issue through sustainable production of an already promising intermediate energy-storage molecule (a semi-stable chemical species which can be used for relatively short-term storage of energy in the form of their chemical bonds), hydrogen peroxide (H_2O_2), using rhodamine derivative tellurium chromophores, most notably 3,6-diamino-9-mesityl-telluroxanthylium (**mesi**) seen in Figure 1.

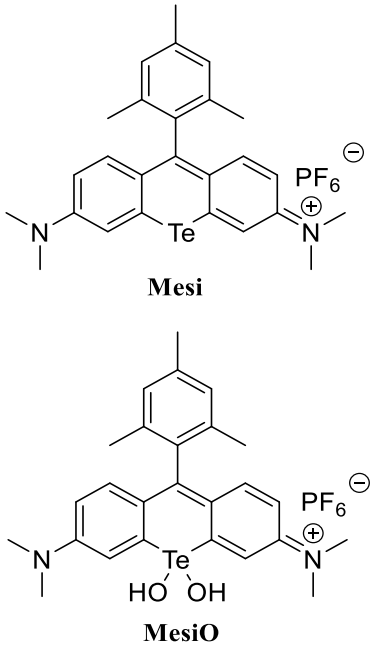

Figure 1: Tellurium-chromophore used in this work, mesi, and its hydrated oxide form, mesiO. All dyes have been obtained from collaboration with Michael R. Detty of the University at Buffalo

Hydrogen peroxide is a molecule capable of performing high energy transformations, commonly used in industrial bleaching applications as well as detergents, antiseptics, and water purification.[4,6–8] It is also well known for its potential use as a propellant in certain rocket technologies.[2,4] Hydrogen peroxide fuel

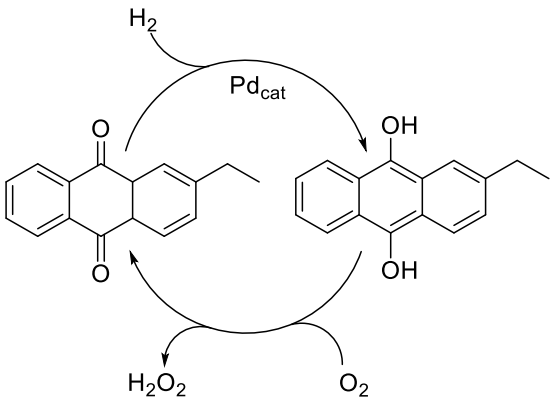

Scheme 1: Simplified Riedl-Pfleiderer process for production of H_2O_2

cells (**PFCs**) can be designed with one-pot electrochemical architectures with power densities and potential output (3.92 $^{MJ}/_{L}$, 1.07 V) comparable to contemporary hydrogen fuel cells (5.11 $^{MJ}/_{L}$, 1.23 V), while at the same time avoiding many of the pitfalls associated with use of H_2 gas.[2] PFCs also have the benefit, as with hydrogen fuel cells, of producing innocuous emissions in the form of O_2 and H_2O vapor, while avoiding the high temperatures that can produce hazardous nitrogen oxides (NO_x) associated with direct combustion hydrogen engines. Currently, 4.3 million tonnes of H_2O_2 are produced annually world-wide, with 95% of it is produced via the anthraquinone process.

The anthraquinone process, seen in Scheme 1, was developed shortly before WWII and though reliable, suffers from a number of costly deficiencies.[6] The cycle's primary catalyst, 2-alkyl-anthraquinone, is dissolved in an alkane solvent mixture and heated to a moderate temperature (>400°C) under pressurized H_2 and O_2 gases. The gases and anthraquinone in the presence of an additional noble metal catalyst (Pt or Pd) react to produce H_2O_2, which is extracted at < 10%w/v aqueous concentrations. The dilute solution must then be reflux-condensed in order to reach the appropriate ~70%w/v concentrations for shipping and industrial applications. The process is fairly energy intensive, carries undue safety risks, and has a relatively high catalyst break-down as a result of the radical chain

reaction responsible for the generation of peroxide. As a method of production for an energy source, the anthraquinone process is unusable. However, it has been determined that tellurorhodamines produce H_2O_2 upon photochemical oxidation in *ambient* conditions, from solvated water and atmospheric O_2, and using relatively low-energy visible light.[9–11]

Tellurium containing rhodamines are unique among the chalcogen-rhodamines due to their self-sensitizing nature. Ground-state triplet oxygen ($^3O_2$) is largely unreactive due to its orbital symmetry, but utilizing energy transfers it can

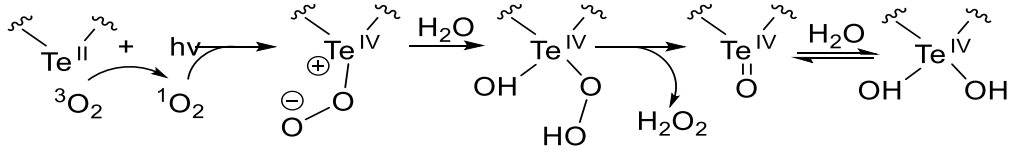

Scheme 2: Photo-oxidation pathway of mesi to mesiO with H_2O and atmospheric O_2

be converted to the reactive form, singlet oxygen ($^1O_2$), to perform useful chemical transofmations. Photosensitizers are molecules whose excited triplet states are able to transfer energy to $^3O_2$. While the other chalcogenides have similar photosensitizing properties to those of tellurorhodamines, generating reactive $^1O_2$ via energy transfer from the sensitizer's excited state to $^3O_2$, the tellurorhodamines can then react with the $^1O_2$ directly, oxidizing the tellurium atom and generating H_2O_2 in the process, as seen in Scheme 2. The telluroxide, in this case **mesiO** in Figure 1, is a reactive molecule that can then be used for specific chemical transformations, such as oxidizing aromatic thiols to disulfides.[10–12] The reduction returns the dye molecule to its original state and is available to undergo photo-oxidation again opening the possibility for the tellurorhodamines to be used as photocatalysts (Scheme 3). In particular, **mesi** is thought to be promising for use as a

catalyst because of the steric stability lent by the methyl groups on its mesityl moiety. Both the process of oxidation and reduction of **mesi** can be monitored via UV-Vis spectrometry, by the shift in the absorbance spectrum between 590 nm and 660 nm, as seen in Figure 2, which can be attributed to the addition to contribution of the hydroxyl groups to the molecular orbitals, specifically lowering the energy gap of the highest occupied molecular orbital (HOMO) and lowest unoccupied molecular orbital (LUMO). There is a well-defined isosbestic point at 620 nm indicating a direct transformation from **mesi** to **mesiO**. However, the turn over number (TON) of **mesi** remains disappointingly low due to catalyst degradation. Competing pathways have been observed indirectly, which indicate that

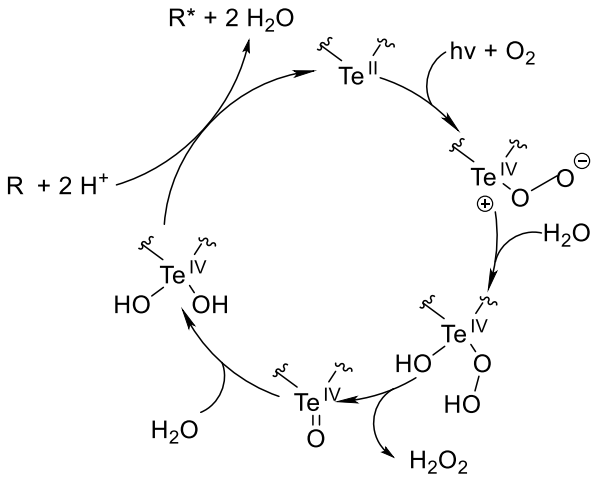

Scheme 3: Direct, substrate-driven catalytic cycle of mesi system

mesi is deactivated both by excessive light exposure and by side-reactions with nucleophilic species in solution. The mesityl derivative, **mesi**, was specifically chosen in order to sterically hinder the suspected mechanisms of degradation, but the strategy has proven minimally effective to that end. The nature of the synthetic by-products and diversity of the products of degradation make it impossible to identify a single majority contributor to the deactivation of **mesi** as a catalyst.

There has been good indication that the dyes are also electrochemically active, due to the dependence of reduction on electronic properties of substrates.[10,11,13] The ability to reduce **mesiO** electrochemically would remove the need for direct mixture of a substrate and catalyst for reduction and would simplify the conditions necessary for production of H_2O_2. Having a system with a catalyst, like **mesi**, to produce H_2O_2 at ambient conditions, using visible light,

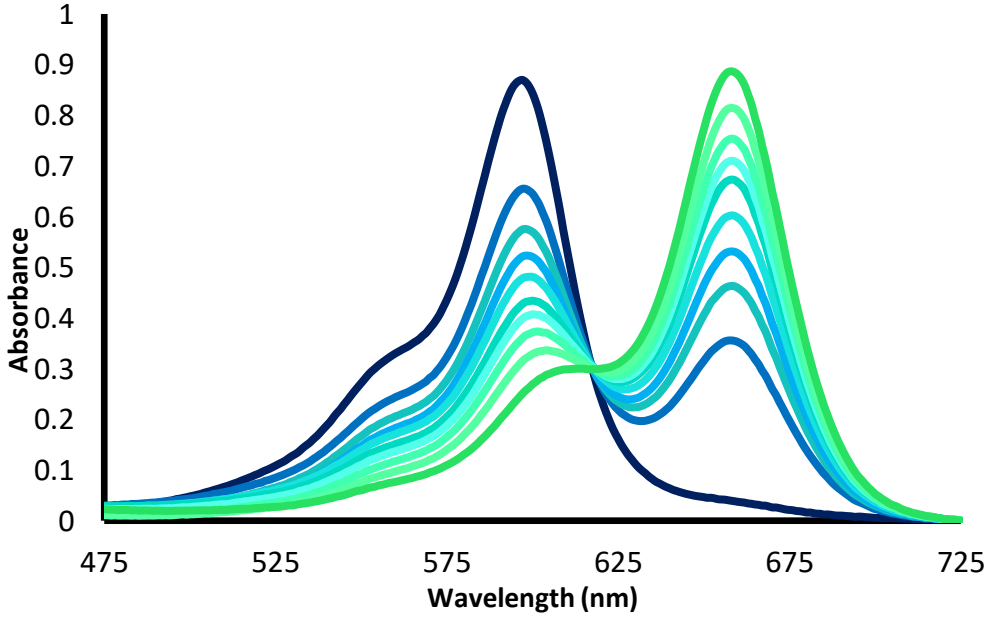

*Figure 2: Time resolved spectra of photo-oxidation over 30 minutes of a 10 µM sample of mesi in 95%methanol/5%water as indicated by dissipation of the peak at 600 nm and growth of the peak at 650 nm. The 95/5% split to facilitate solubility of **mesi** while providing an adequate amount of water to limit degradation and speed oxidation in accordance with scheme2*

atmospheric O_2, and water would provide significant industrial improvement over the anthraquinone process, possibly allowing H_2O_2 to be used as a fuel source.

1.2 Photocatalysis

Photon driven catalysis is desirable and a heavily researched topic in chemistry and material sciences in general. The concept of using chemical systems to transfer energy from light to perform chemical transformations is both

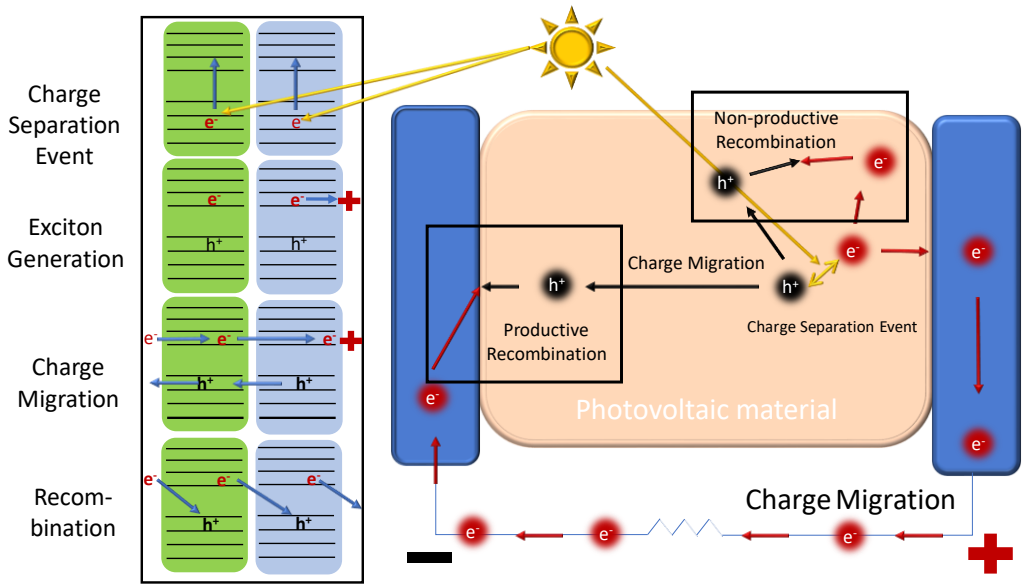

Figure 3: Simplified diagram of exciton generation and recombination in heterojunction photovoltaics; extended orbitals of adjacent atoms represented by green and blue coloring

ecologically and economically favorable to many contemporary stoichiometric chemical processing methods. Though there is a lot of variation in the target molecules and mechanisms by which catalysis occurs, in terms of structural kinetics and electronic properties, most photocatalytic activity hinges on generation of excitons; quasiparticles made up of an electron (e^-) in an excited state, and the positively charged vacancy left from the excitation event, commonly referred to as a 'hole'(h^+) as seen in Figure 3. Though perhaps overly simplified, the extended

orbitals created by semi-conductor photovoltaics illustrated in Figure 3 are responsible for the separation and migration of the e^- and h^+ excitons. This precarious separation is often eliminated through non-productive recombination; that is, when an e^- and h^+ recombine without traveling to and passing through the intended circuit load to perform work. High rates of recombination correlate to low solar efficientcies of photo-systems in general.

A large body of research is focused on heterogeneous catalysis using solid, bulk catalysts such as TiO_2, ZrO_2, and WO_3. These methods have the advantages of distinct phase separation, stability, and wide substrate scope (with the exception of perovskites).[14–20] However, heterogeneous photocatalysts generally suffer from inconsistent reaction rates and sluggish reaction kinetics, most often attributed to e^--h^+ separation and relatively high rates of recombination. Homogeneous photocatalysts, exemplified by compounds such as *tris*(bipyridine) ruthenium(II/III) and various metal-porphyrin complexes, somewhat improve on those issues by increasing reaction-surface area within a liquid solvent matrix. This can result in extension of exciton life times from the femto/picosecond regime into the nanosecond and in some cases even in to the microsecond regime.[21–25] Though there are some characteristics that differentiate the excited states of homogeneous photocatalysts from excitons induced in solid-state heterogeneous photocatalysts, the concepts are fundamentally linked. Combinations of the two approaches have been pursued to great lengths in order to account for the short-comings of each individual method for decades, but has the field experienced considerable

acceleration since 1988, during which development of dye-sensitized solar cells (DSSC) became prevalent.[26–29]

Rhodamines, seen in Figure 4, as well as other chalcogen-containing derivatives, fall into a broad category of photocatalytic molecules known as photosensitizers. This class of molecule absorbs photons and transfers the energy, usually through Förster Resonance Energy Transfer (FRET), to other molecules that participate directly in the chemical transformation of interest. In heterogenous-hybrid photocatalysis the FRET mechanism is replaced by electron exchange of small molecules with the bulk catalyst material, and the energetic minutia, both thermal and kinetic effects, arising from the difference in pathways (migration of charge carriers versus energy exchange via resonance) is often responsible for

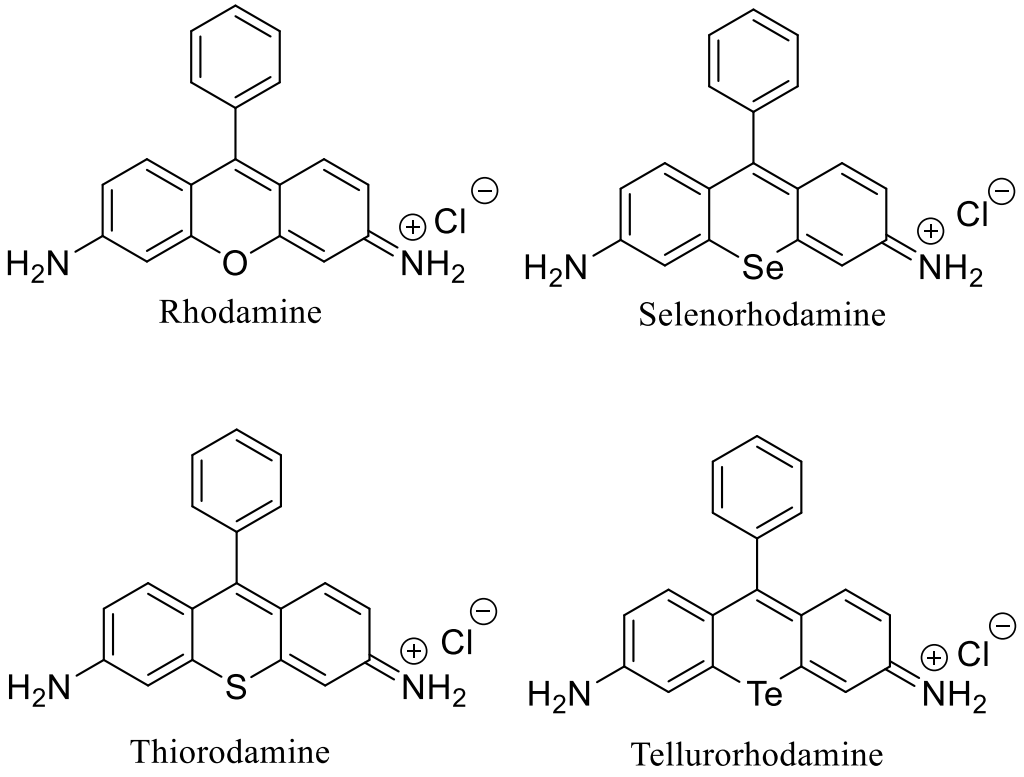

Figure 4: Rhodamine and its basic chalcogenide derivatives

continued deficiencies in the overall approach.[14,27,30] The transfer in energy in FRET mechanisms are much faster with lower energetic barriers than through-space electron exchange, but are also nearly impossible to direct in a way that facilitates generation of an electric current or to perform mechanical work. While photosensitizers are a class of molecules that are of interest to development of heterojunction technologies like DSSC's, **mesi** and other tellurium containing derivatives differ from molecules containing the lower-period chalcogens (O,S,Se) in that, they are "self-sensitizing". The presence of a tellurium atom changes the reactivity of the molecule as compared to the other chalcogens, and the sensitizing molecule itself becomes directly involved in the reaction. The energy from the excitation is transferred to the $^3O_2$ via FRET mechanism much the same as typical photosensitizers. However, the resultant $^1O_2$ then reacts with the tellurorhodamine directly, rather than reacting with a third-party molecule (Scheme 2). Photo-oxidation of **mesi** to **mesiO** is beneficial in terms of energy storage not only due to production of H_2O_2, but also as it constitutes a sort of energy storage via the tellurorhodamine itself; **mesiO** can be used as a stoichiometric oxidant. This self-sensitizing quality of the tellurorhodamines allows them to perform chemical transformations in aerobic environments, removing the need for co-catalysts typically seen in other photocatalytic systems.

1.3 Photoelectrochemical Electrodes

Much of the field of solar energy conversion is devoted to investigation of photovoltaic materials, or hybrid approaches as discussed with DSSC technologies. Semi-conductor materials, such as those mentioned as photocatalysts in the

previous section, as well as noble metals and nanomaterials, are being investigated for direct conversion of solar energy into electricity.[31–35] While developments have made photovoltaic solar energy economically viable with modest efficiencies, current technologies fail to address a key issue with photovoltaic approaches to energy, the issue of storage. Photoelectrochemical methods hold the promise of addressing this issue.

The most common approach to chemically storing solar energy is via water electrolysis, which can be divided into two steps: water oxidation reactions (WOR) and hydrogen reduction reactions (HRR). As can be seen in Figure 5, the set of reactions produce O_2 and H_2 gas from water through electrolysis with energy converted by a solid-state heterojunction via direct or indirect solar energy input. The process is highly desirable since the primary reagent is water, and H_2

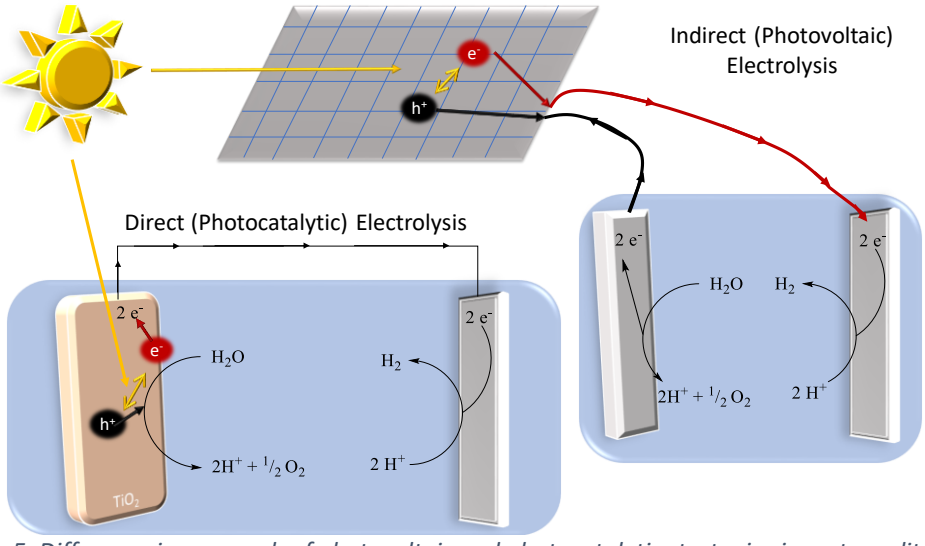

Figure 5: Difference in approach of photovoltaic and photocatalytic strategies in water splitting for solar energy storage. Indirect electrolysis uses electromotive force supplied by an external system to drive WORs, whereas direct electrolysis uses the photocatalysis of WOR to facilitate its electromotive force

has the highest known energy density of any potential fuel source, even when

accounting for compression.[2,36] The difficulty in application of water electrolysis comes from the relatively high energy input required for the WOR, which is known for its troublesome chemical kinetics. Despite the difficulty many photoelectrochemical systems focus on development of anodes with the specific aim of enhancing that oxidation.[14,32,35,37–39]

However, there are approaches being explored for solar energy storage with photoelectrochemical cells based on reactions other than water electrolysis. Most of those processes revolve around reduction of carbon dioxide (CO_2) to fuels like methanol (MeOH) and methane (CH_4), or into chemical feedstocks like carbon monoxide (CO) and acetic acid (CH_3COOH).[18,40–43] Other processes are quite innovative in their approach, as with the work done by Shanmugam *et al*, which utilized controlled/living radical polymerization (CLRP) in a cathode, combining light driven and light inhibited processes within the photoelectrochemical cell to generate complex macromolecules.[44]

Use of tellurorhodamines is a bit more direct than any of the aforementioned approaches, as both CLRP and CO_2 reduction call for highly specialized bulk materials, WOR/HRR is highly energy intensive, and all have rather poor energetic yields at this point in time.[18,40–44] By pairing the photochemical and electrochemical properties of the **mesi** and **mesiO** respectively, one can construct a viable half-cell. The system can comprise a photoelectrochemical cathode in which **mesi** is photo-oxidized so that **mesiO** can be electrochemically reduced as part of an electrochemical cell ($E_{cell} = E_{cathode} - E_{anode}$). The ability to generate a

working current from the photoelectrochemical cell while simultaneously producing an energy storage molecule is, so far, unique to the proposed **mesiO** cathode. Most approaches, in terms of photoelectrochemical cathode or anode, focus on the solar-energy input to drive the underlying chemistry, but due to the reactivity of **mesiO** it is possible to generate a working current with a complimentary half-cell, while simultaneously producing H_2O_2 catalytically for use later in PFCs. If implemented on a broad scale, after sufficient development and pairing with a compatible photochemical anode, an approach such as the **mesiO** cathode would represent a significant step in addressing the fundamental short-coming of current solar-energy technology as well as providing a path to relief of growing energy demand.

2. Experimental

2.1 Materials

All 3,6-diamino-9-mesityl-telluroxanthylium used was available in the lab, prepared according to De Valle *et al*.[45] With the exception of de-ionized water produced on site, solvents used in experimentation were Sigma-Aldrich supplied unless otherwise specified: acetonitrile >99% HPLC grade cas 75-05-8, methanol >99% ACS certified cas 86-78-1, and propylene carbonate (**PC**) (TCI) >98% electrochemical grade cas 203-572-1. Buffers were prepared from sodium acetate (BDH VWR Analytical, ACS certified, IN#BDH-927-500), phthalic acid (Matheson Colonel & Bellfact chemists technical grade), sodium phosphate (available from stock supply), and sodium borate (Mallinkraft, analytical grade, 7460) titrated with prepared solutions of hydrochloric acid (Sigma-Aldrich 37% ACS certified SHBJ3023) or sodium hydroxide (Sigma-Aldrich >98% SLBF2381V) to the appropriate pH, then diluted to the desired concentration for stream-lined standardization of buffers. Organic electrolytes tetra-n-butyl ammonium tetra-fluoroborate (**TBAFB**) (Southwest Analytical Chemicals Inc, electrochemical grade, IN#5204) and tetra-n-butyl ammonium fluoride (**TBAF**) (TCI >98% cas 22206-57-1) were used in electrochemistry experiments. Quantification of hydrogen peroxide was carried out using stock solutions of H_2O_2 (Fisher Chemicals 30% ACS certified cas 7737-18-5), perchloric acid (Fisher chemicals 60% ACS certified cas 7601-90-3), and Oxo [5, 10, 15, 20-tetra (4-pyridyl) porphyrinato] titanium(IV) (**Ti-Pphy**) available in the lab prepared by the method described by Inamo *et al*.[46]

2.2 Instrumentation

Visual spectral data was collected with a Shimadzu UV-VIS-NIR Spectrophotometer UV-3600. Spectroelectroelectrochemistry experimentsutilized a StellarNet INC, Spectrawiz spectrometer SL5 source and Spectrawiz Silver Nova 75 detector for the instrument's ability to provide real-time (instantaneous and time-resolved, rather than event-driven or sequential) readout of sample spectra. Electrochemical data were collected with a BioLogic Science Instruments potentiostat SP-200. All water and atmosphere excluding processes were carried out in an mBraun Glovebox Unilab 1950/710. Gaseous mass analysis for O_2 content was accomplished with a Hiden Analytical benchtop gas analysis system HPR-20 QIC. Light sources included hand-lamps lit with varying compact fluorescent bulbs, single phosphor coated light-emitting diode (LED) light sources, as well as circular, multi-LED arrays for bulk oxidation.

2.3 MesiO Isolation

While **mesi** samples were prepared directly from a solid tellurorhodamine, **mesiO** samples were prepared from photooxidation of a portion of **mesi** within the same solutions. For many experiments though, it was necessary to isolate **mesiO** from the reaction mixture to remove the effects of H_2O_2. The high reactivity of H_2O_2 with certain solvents, substrates, and **mesi** itself makes its presence a problematic for many types of measurement, making results difficult, or in some cases impossible, to interpret. These samples were prepared in 99:1 methanol/water mixtures at roughly 100X dilution of the desired concentration, photooxidized with broad-band sources, concentrated via rotovapping, then once a

minimal volume was achieved, they were exposed to a moderate airflow over a room-temperature water-bath until dry. The isolated samples were typically stored in a desiccator overnight, until reconstituted or moved into the glovebox for further preparation.

2.4 Electrochemistry

Samples for electrochemical experiments were typically prepared of **mesi** or **mesiO** in PC with 0.1 M TBAFB. However, the tetrafluoroborate ion (BF_4^-) was found to catalyze WORs and fluorination that obscured voltammograms; these specific conditions result in traces dominated by mechanisms of WORs, hiding the behavior of the actual target analytes. Samples prepared with significant concentrations of water, and so TBAF was substituted for differential pulse voltammetry (DPV) and certain cyclic voltammetry (CV) experiments.

All open-circuit voltammetry (OCV), CV, and DPV were performed with a Pt button working electrode and Pt wire counter electrode were employed alongside a Ag/Ag^+ organic reference electrode. Though use of Ag/AgCl reference electrodes has become the standard in electrochemical experiments, organic solvents like PC require the use of augmented references, the most reliable of which has been found to be silver wire in a solution of silver nitrate ($AgNO_3$), which forms the Ag/Ag^+ electrode. Water was added up to 10%v/v to the sample to facilitate oxidation where necessary. Spectroelectrochemistry (SEC) was carried out in a specialized cuvette with Pt wire for both working and counter electrodes. The SEC experiments were carried out in the absence of a reference electrode due to

spatial limitations; voltages were approximated by measuring a spike of Ferrocene after the experiment was complete.

2.5 H_2O_2 Detection

2.5.1 UV-Vis Quantification

In pristene **mesi** solutions, H_2O_2 can be quantified post-oxidation using a method described by Matsubata *et al*. By preparing samples of a set concentration of **mesi** (12.0 μM) with standarized solutions of H_2O_2 from stock, Matsubata's method can be used to calibrate the system of mixtures of **mesi** and **mesiO** for quantification; mixed systems of the two forms of tellurorhodamine will be referred to as "**mesi/O**" to distiguish from solutions focusing on the presence of either **mesi** *or* **mesiO**.[47] Standard solutions were mixed 1:1:1 with 15 μM Ti-Pphy and 6 M $HClO_4$, and allowed to react for one minute before being scanned via UV-Vis for a decrease in absorbance at 432 nm. This quantification can only be acchomplished for initial oxidation of the solutions, as attempts to quantify H_2O_2 in cycling of **mesi** have proven difficult and inconsistent due to the complexity of the interactions of **mesi** and H_2O_2 in solution. The result of the calibration has a very reasonable correlation, as seen in section 4.2.1.

2.5.2 Headspace Analysis

Headspace analysis was also used to gauge the presence of H_2O_2 in the **mesi/O** system. Isolated **mesiO** was reconsituted to a concentration of 1.0 mM in PC in a glovebox, and the resulting solution was split between round-bottom (RB) flasks and open vials. After being removed from the glovebox, one set of sealed and open samples was reduced thermally in an oil bath at a temperature of 80ºC

until fully reduced. The other set was electrochemically reduced with Pt wire electrodes, which had been passed through the air-tight septum before removal from the glovebox for the air-tight sample. The open-air, parallel samples were monitored via UV-Vis to approximate the stage of reduction of the sealed samples.

Once fully reduced, the sealed samples' headspace were measured with the bench-top mass analyzer for O_2 content, using an improvised N_2 inert-gas-line as a delivery system. The inert-gas-line consisted of tubing and stopcock valves held up by a ring stand; the 'reading' chamber consisted of a low-volume RB-flask to which the analyzer was attached, as well as the oil-bubbler-outlet, and sampling and control lines. The sampling line was a short tube with an on/off stopcock valve to be connected to the sample flasks. The control line, used to flush the system, was connected to a 3-way stopcock valve, which regulated the N_2 flow between the source tank, the control line, and the mobile line. The mobile line ran from the 3-way stopcock to be attached to the sample so that the headspace of the sample could be pushed into the reading chamber. To flush the system before measurments began, all stopcocks were open and the N_2 allowed to flow through the system for 5 min. After flushing, the sample line was closed and the flow was stopped to the mobile and control lines, and a sample flask hooked into the system. The N_2 flow was restored to the mobile line, and the analyzer was allowed to take a base-line of the system, while the N_2 flow was regulated to a minimal rate, evaluated by the bubbler. Once the bubbler rate had stabilized the control line was closed and the mobile line was opened, then the sample stopcock

opened (sample injection) and the analysis began. Peaks, where present, were observed after an apporximate 3 second delay, correlating well to sample ‘injection’, as seen in section 4.2.3. Each sample and control was treated as similarly as allowed by the improvised set-up.

3. Characterization of Mesi as a Photoelectrochemical Cathode

3.1 Photocathode Introduction

It has been well documented that tellurium containing chromophores, such as **mesi**, are readily oxidized by $^1O_2$, following photoexcitation and energy transfer, as proposed in Scheme 2.[10,11] Previous work has also shown that once oxidized, the chromophore is also able to facilitate various potentially useful chemical transformations, such as oxidation of thiols to disulfides, and work published by our research lab has shown that those chemical transformations can be carried out catalytically. However, despite advancements in understanding the system, the problem plaguing these catalytic cycles is that the tellurium containing chromophores tend to break down rapidly in the presence of substrate. In order to

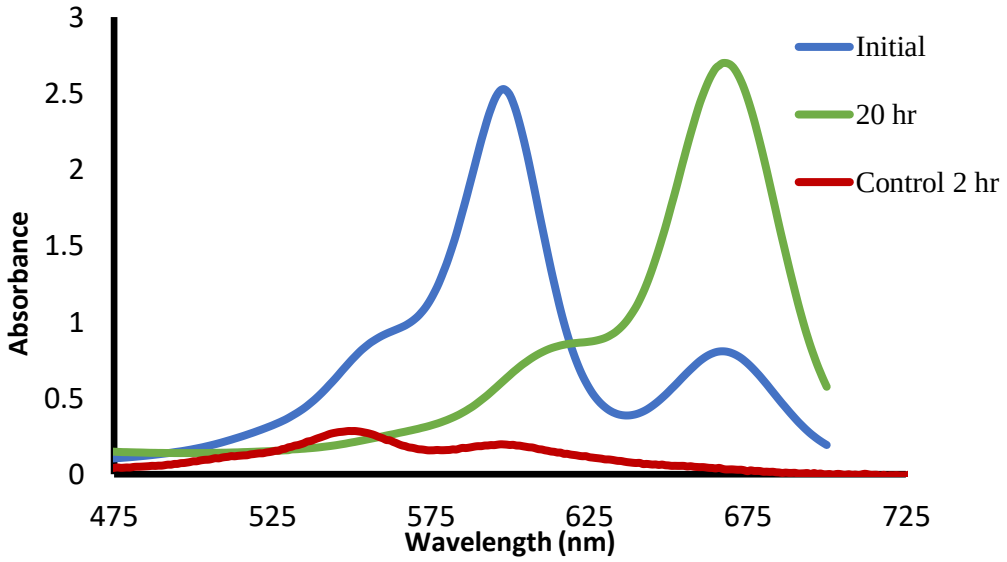

Figure 6: Photo-oxidation of 30 µM samples of mesi in 10% methanol solutions with 1.0 M urea (green) and without urea (red). Initial samples were partially oxidized by errant light during preparation, speaking to the sensitivity of these solutions

improve the potential catalytic applications of tellurorhodamines, finding a route by which the catalytic activity of the dye is preserved while avoiding rapid degradation is necessary.

Some success has been found by control of additives. In Figure 6, it can be seen that solutions of **mesi** in partially organic solvents, which usually degrade within 2 hours of illumination, can be protected by application of urea as an additive. The mechanism of this protection is still unknown, but samples have been preserved in activity and population for up to and beyond 20 hours as a result of the addition of urea. A similar effect can be shown by the pH dependence of the system observed in Figure 7. The trend of oxidation in acidic conditions (Figure 7.A) sees **mesiO**

A.

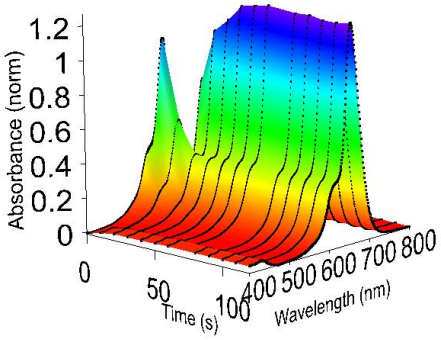

B.

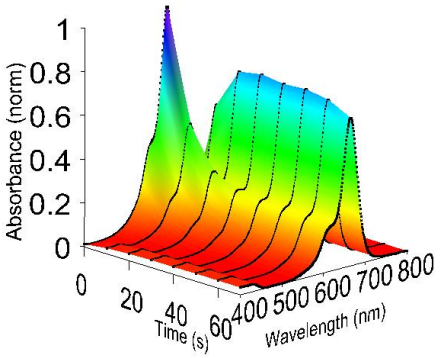

C.

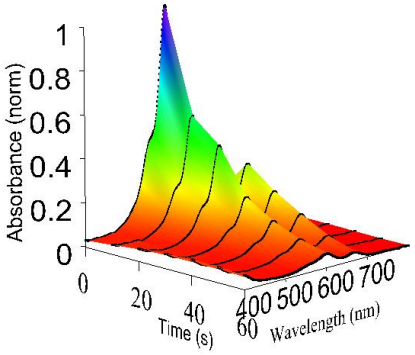

Figure 7: Time-resolved, normalized spectra of the photo-oxidation of 10 µM mesi samples in 50% methanol with A) 1.0 M acetate buffer at pH 4, B) 1.0 M phosphate buffer at pH 7, and C) 1.0 M borate buffer at pH 9. The color gradient is purely indicative of absorbance intensity relative to the spectral maximum

forming quickly and showing no sign of degradation as indicated by the change of the peak at 650 nm over time. In even neutral solutions (Figure 7.B) **mesiO** does not form completely and even starts to decline toward at time scales past 60 seconds. In alkaline media (Figure 7.C) both **mesi** and **mesiO** can be seen to degrade under 60 seconds as indicated by the diminishing absorbance intensities at both 600 and 650 nm.

While degradation has been observed as a result of excessive light-exposure, the 'over-oxidation' caused by photo-excitation can be slowed and even prevented by control of factors including the solvent-matrix composition (as illustrated with the addition of urea Figure 6), pH (indicated by the rapid degradation visible in Figure 7), and temperature. In the presence of substrate there has not yet been a reliable method found for prevention of catalyst break-down. It is possible that the solution to substrate driven degradation of the catalyst could be found in an electrochemical approach. The observed scope of thiol oxidation reported previously suggests that the electronic properties of the substrates are largely responsible for the observed reactivity, with aromatic thiols being readily oxidized and aliphatic thiols showing little or no reaction.[11] Chalcogens, particularly sulfur, are well known for their ability to participate in outer-sphere electron transfer, so it is reasonable to believe that the redox chemistry observed between the tellurium containing catalyst and aromatic thiol compounds could be achievable through electrochemical methods.[48–52] When the electrons for reduction of the catalyst are supplied by an electrode rather than directly from a substrate, the risk of degradation of the catalyst should be minimized. The electrochemical properties of

these tellurorhodamine chromophores have not been previously explored and initial testing has shown some promise to a photoelectrochemical approach to catalysis. This thesis describes an investigation into the system proposed in Figure 8, in which **mesi,** following energy exchange from incident light, is oxidized in the presence of O_2, H_2O, and a source of H^+, resulting in formation of H_2O_2 and **mesiO**, the latter of which can then be reduced on the electrode to regenerate **mesi** for subsequent turns of the catalytic cycle, while simultaneously generating a working-current.

3.2 Electrochemistry

3.2.1 Cyclic Voltammetry

Cyclic voltammograms (CVs) were collected of **mesi** and **mesiO** at 10 mM concentrations in propylene carbonate (PC) with 0.1 M tetra-butyl ammonium fluoroborate (TBAFB) as the electrolyte. The potentials have been corrected

to the standard hydrogen electrode (**SHE**), the equivalent potential standard corresponding to $\Delta G = 0.0$ kJ on the free energy scale, for ease of reference to other electrochemical and thermodynamic systems. Scan rates and potential windows for the potentials applied between working and counter electrodes in the systems were narrowed to eliminate the exponential behavior indicating solvent breakdown, the limit of the observable electrochemical processes within the samples. The resultant voltammograms can be seen in Figure 9. As the potential is changed influx of negative of currents correspond to oxidative processes occurring around the working electrode, while influx of positive currents is indicative of reduction events. The voltammograms have been presented using the 'Texas convention' (potentials becoming

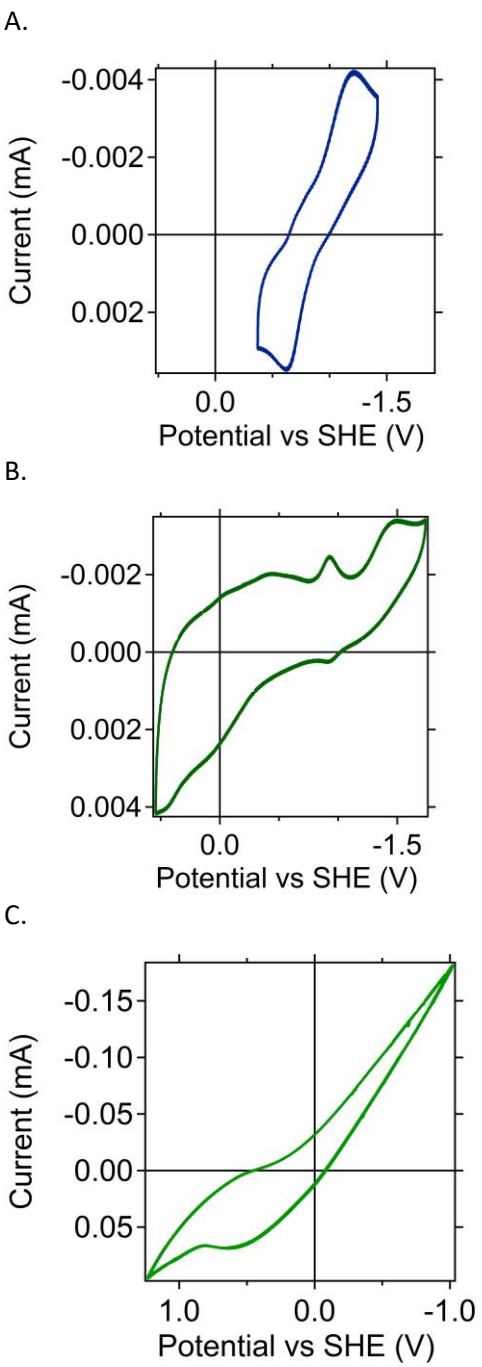

Figure 8: Cyclic voltammograms collected at 750 mV/s with Pt button and Pt wire working and counter electrodes respectively, of samples in propylene carbonate with 0.1 M TBAFB A) 0.1 mM mesi, B) 0.1 mM mesiO prepared from oxidation of A, and C) 0.1 mM mesiO carefully isolated and reconstituted in air-free, water-free conditions with 0.1 M TBAF

more negative left to right, and currents becoming more negative bottom to top), as is the common practice for cathodic systems.

The **mesi** profile in Figure 9.A indicates a single, reversible reduction event, with a single reduction peak around - 0.63 V corresponding to the current maximum, while an oxidation event can be seen at -1.21 V corresponding to the current minimum. While there is curvature suggesting that other redox events may be present, the apparent 580 mV peak separation indicated a non-Nernstian relationship. The magnitude of the separation in peaks between corresponding electrochemical events in Figure 9.A with respect to the potentials at the minimum and maximum currents indicated a significant kinetic limitation to the process when compared to the expected 59 mV per electron separation in Nernstian systems.

MesiO appears to have a profile much more suitable to cathodic application as indicated by Figure 9.B&C. The profile observable in Figure 9.B implies significant interference from H_2O_2 and so **mesiO** was isolated from the rest of the sample preparation solution, as described in section 2.3, in order to collect the 'clean' voltammogram seen in Figure 9.C. A broad peak is present as a shoulder at +0.44 V in the lower left-hand quadrant of Figure 9.B, though the processes are again non-Nernstian likely due to complication from kinetic processes at the electrode surface, and can be correlated to the singular peak of the isolated sample in Figure 9.C. Interestingly, the oxidative process observed in Figure 9.B at -0.92 V has a subdued, but visible reduction event at -0.87 V indicating a single electron

transfer by virtue of its ~59 mV peak separation, in keeping with Nernstian electrochemical behavior. The event corresponds well to the known potential of a perhydroxyl radical ($HO_2^{\bullet -}$) and further indicates the interference of H_2O_2 in the sample prepared for Figure 9.B.[53–55] The presence of those peaks are a strong indication that H_2O_2 was produced upon photooxidation and contributes to the CV profile.

3.2.2 Differential Pulse Voltammetry

To account for kinetic effects within the **mesi** and **mesiO** systems, differential pulse voltammetry (DPV) was performed. By examining the minute changes in current before and after pulses in potential, changes in diffusion and reaction kinetics can be overcome within electrochemical systems, though there is a loss in the ability to resolve cathodic and anodic processes. The combination of information from CV and DPV techniques should yield the most pertinent electrochemical characteristics of the tellurorhodamine system.

Isolated **mesiO, prepared according to section 2.3,** was reconstituted in dry, degassed PC for DPV sample preparation. All samples were collected with an equivalent sweep-rate of 750 mV/s. The samples were spiked with water to 10%v/v composition, after anhydrous readings were taken. This was done to observe the effect of water on the system with respect to Scheme 2.

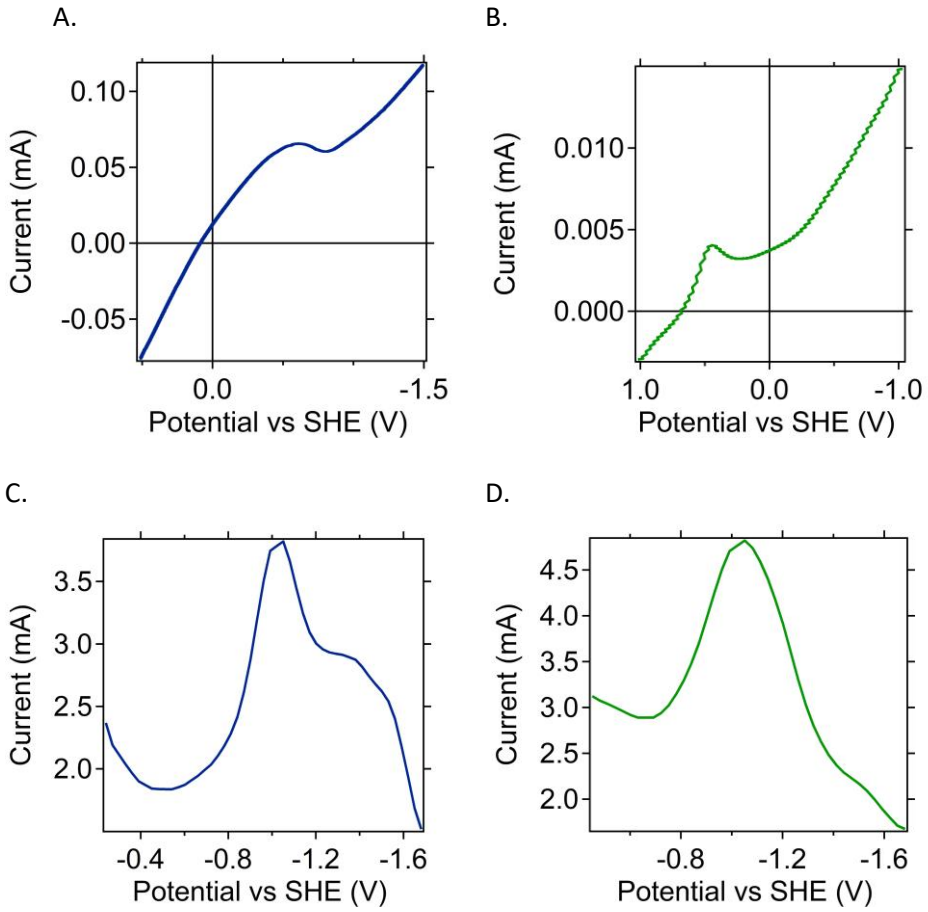

Figure 9:Differential pulse poltammograms collected at effective scan rates of 500 mV/s with Pt button and Pt wire working and counter electrodes respectively, of samples in propylene carbonate with 0.1 M TBAF and A) 0.01 M mesi, B) 0.01 M mesiO, C) 0.01 mM mesi with 10%v/v water, and D) 0.01 mM mesiO with 10%v/v water

3.2.3 Electrochemical Results & Discussion

Though information is lost between CV and DPV techniques, the information in the voltammograms in Figure 10 is consistent with what was observed in the CV experiments. The absence peaks in Figure 9.C indicates that the H_2O_2

was successfully removed from the system, as the multitude of peaks which were observed in Figure 9.B are indicative of a wide variety of electrochemical events including the characteristic $HO_2^{\bullet -}$ peak. Though difficult to see, the peak corresponding to +0.44 V in Figure 9.C and 10.B indicating the reduction event can also be seen in Figure 9.B, present as a shoulder of the **mesiO** trace. The presence of that peak in both voltammograms indicates that the reduction event can in fact be attributed to **mesiO**. The difficulty in resolving the peak in Figure 10.B is likely due to the difference in DPV and CV in terms of their sensitivity to solvent-breakdown effects. The distinct lack of additional peaks in both Figure 9.C and Figure 10.B implies that it is likely the reduction of **mesiO** is not electrochemically reversible in the anhydrous samples.

The **mesi** trace, Figure 10.A, is also consistent with the corresponding CV, Figure 9.A. The large peak separation visible in Figure 9.A, and slight dip visible in the peak at -0.63 V could be an indication of the expected 2 electron transfer as would be expected from the **mesi** to **mesiO** oxidation (Te^{2+} to Te^{+4}, rather than Te^{2+} to Te^{+3}), though attempts to further resolve the peak were unsuccessful. The duel peak feature is better defined, though still unresolved, in the samples spiked with water, Figure 10.C&D. Though the peaks are more prominent in the **mesiO** sample, Figure 10.D, the expected double peak can be seen in both samples, corresponding well to the expected -1.23 V for water oxidation allowing for shifting due to solvent effects. Though water oxidation is a four-electron process, the double peak is expected because the rate limiting step in water oxidation is a double electron transfer step.

Of greater interest within this system is the oxidation peak present in both **mesi** samples at -1.50 V, but absent from both **mesiO** samples. In fact, the peak becomes much more prominent in the sample when the water spike is added. The presence of that peak in Figure 10.C and absence from Figure 10.D, plus the absence of reversibility in Figure 9.Cseems to further validate Scheme 2 in terms of the instrumental role that water plays in oxidation of **mesi** and hydration of the telluroxide to form **mesiO**, but also provides some evidence that the photochemical and electrochemical mechanisms of the system may be linked. A connection between photochemcial and electrochemical properties of the system implies a significant potential for the system to be used as a photoelectrochemical half-cell.

3.3 Photoresponse

3.3.1 Spectroelectrochemistry

The next logical steps in assessment of a system as a photoelectrochemical half-cell is direct observation of the connection between photochemical and electrochemical processes; approaching the issue energetically both from a photophysical and a potentiometric direction. There are two methods of assessment in these cases, both of which have been pursued in this work. Spectroelectrochemistry (SEC) is a technique in which a static, electric potential is applied to a sample while the UV-Vis spectrum of the sample is observed; any changes which occurred within the sample are attributed to the energy provided by the electric potential. Conversely open-current voltage (OCV) experiments examine the variability of a sample's electronic potential under external stress by measuring the potential difference between the working and counter electrode over time, as

compared to the reference. In this case light was providing the external energy, while any resultant electrochemical changes were signified by fluctuation in the measured half-cell potential. By combining these two techniques the true potential of the system as a photoelectrochemical cathode should become apparent, as the link between the photocatalytic properties and the redox-active chemical properties is probed.

A sample of isolated **mesiO** was dispensed into a specialized SEC cuvette with platinum wire working and counter electrodes. A reference electrode was not used due to limitations of the space within the cuvette and, as such, voltages used were relative and unable to be correlated to meaningful potentials. The potentials were chosen on the basis of indicators given by the potentiostat thatoxidation or reduction were occurring. Care was taken to ensure that the potentials used did

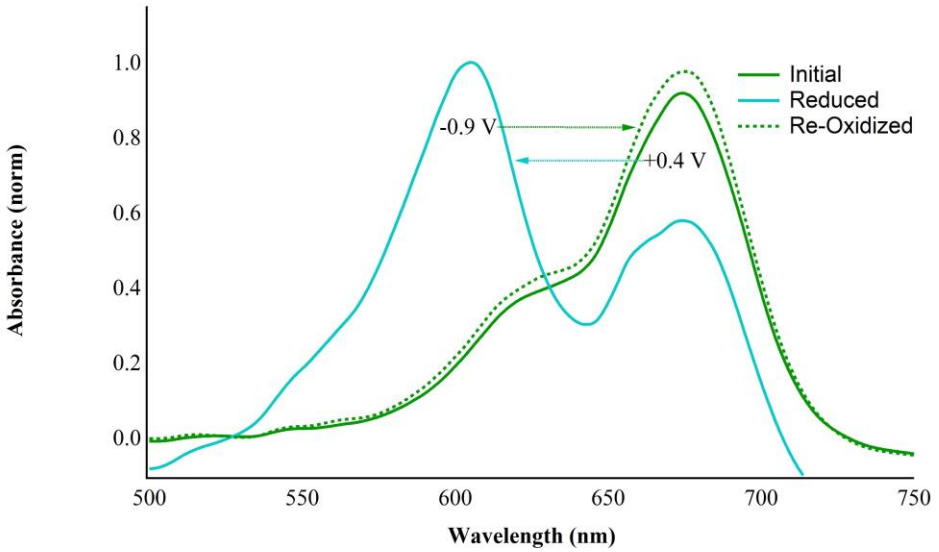

Figure 10: Normalized absorbance spectra of a sample of mesiO in propylene carbonate with 0.1 M TBAF held at reducing and oxidizing potentials for up to 1.5 hrs to show purely electrochemical control of the mesi/O catalytic cycle; arrows indicative of the shift in the spectrum of the sample over time

not induce solvent break-down as evidenced by the monitoring the magnitude of the current. The UV-Vis spectrum of the sample was monitored throughout the application of different potentials over the course of several hours. The sample was first reduced with a strong positive potential successfully generating the telluride form of the catalyst, as evidenced by the dissipation of the absorbance peak at 670 nm in Figure 11, and growth of the peak at 600 nm corresponding to **mesi**. Upon application of an oxidizing potential, the reverse process was observed, a dissipation of the 600 nm peak and recurrence of the absorbance peak at 670 nm, indicating the formation of **mesiO**.

3.3.2 Open-Current Voltage

The SEC experiment demonstrates that the oxidation of the tellurorhodamine can be accomplished through strictly electrochemical means, removing the need for the catalyst to be in direct contact with substrate. However, the question remained as to whether or not the system can produce a usable potential as a result of the connection between electrochemical and photochemical properties, as suggested by the results of CV and DVP. In order to assess the viability of the

tellurorhodamine system as a photoelectrochemical cathode, OCV measurments were taken.

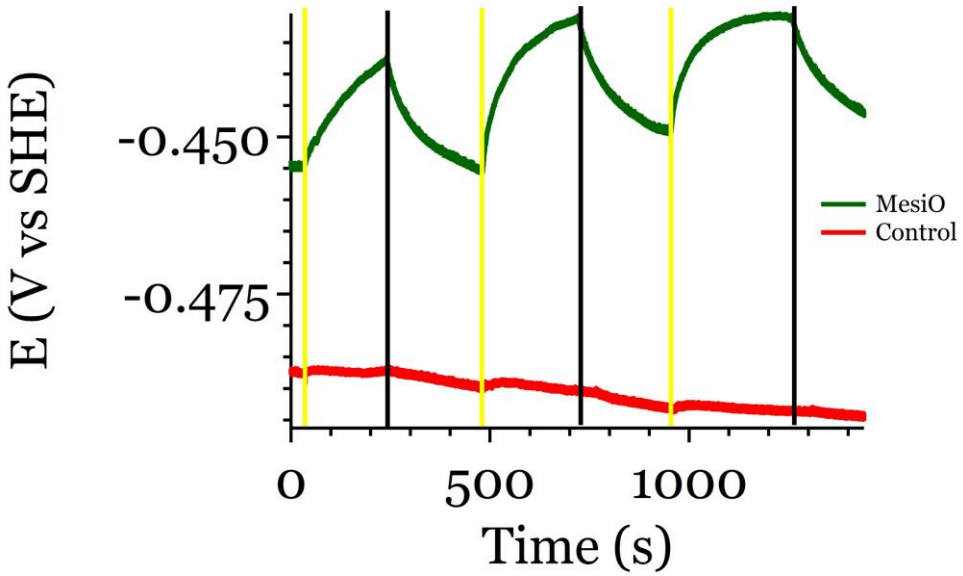

Figure 11: Open-circuit voltammogram of 0.01 mM mesiO in propylene carbonate with 0.1 M TBAF (green) and a control of propylene carbonate and 0.1 M TBAF (red). Both samples were irradiated with a broadband light source for 4 min intervals (yellow – lights on ; black – a lights off) within a light excluding apparatus

The sample and electrodes were set in a light-excluding apparatus equipped with a white LED light source in the bottom. The sample was illuminated for 4-minute intervals and allowed to discharge for the same time while the OCV was monitored. An identical sample was prepared and treated in the same manner, expect with the absence of the tellurorhodamine. Though there is some drifting of potential in the control, there is no correlation to the light source as seen in Figure 12.

3.3.3 Photoresponse Results & Discussion

The **mesiO** sample shows a small yet significant shift in potential directly corresponding to fluctuations in availability of incident light. The potential of the

tellurorhodamine seems to plateau at -0.435 V after starting at -0.455 V. The plateau observed is believed to be caused by saturation of the redox active **mesiO** around the electrodes and seems to indicate that the electrochemical reduction occurs at a slower rate than the photochemical oxidation.

Electrochemical reversibility of tellurorhodamines in the absence of peroxide species is an excellent signifier of a greater potential for photoelectrochemical applications. Many photoelectrochemical electrodes, especially those aimed at photocatalysis of a target molecule, are designed solely to lower activation energy of the desired process; e.g. water oxidation cells are developed to use the light energy and electrochemical potential to produce H_2 for later use, not for direct production of a *working* current. Such half-cells are paired favorably to overcome high energy transitions like those found in WOR, but are rarely observed for have favorable reduction potentials for *in-situ* current generation. However, the results of the OCV paired with SEC show that is not the case for the **mesi/O** half-cell, which can both produce a storage molecule at the same time as it produces a working current that could be used to power external or auxiliary devices.

The potential difference observed as a result of the system's access to light may be modest, but given the sub-millimolar concentrations in testing, even that modest differential is sufficient to suggest that the tellurorhodamine is suitable for use in a photoelectrochemical system. With greater concentrations of **mesi** in solution, the system should be able to reach a maximum half-cell potential of +0.44 V as indicated by the mesiO voltammograms in Figures 9.C & 10.B

corresponding to the suspected reduction event responsible for **mesiO** reduction, before discharging to a theoretical minimum of -0.56 V signified by the anodic current seen in Figure 10.A, as the suspected oxidation event responsible for oxidation of **mesi.**.

4. Investigation of the Photoelectrochemical Production of H_2O_2 by Mesi

4.1 Peroxide Introduction

The primary interest in construction of a photoelectrochemical half-cell using **mesi** comes from the dye's tendency to produce H_2O_2 upon photo-oxidation. What is currently known about mechanism is that the generation of H_2O_2 in the **mesi** solutions occurs at room temperature and pressure, in aqueous solutions, and using atmospheric O_2 and H_2O as reactants. As opposed to other known catalysts, **mesi** also undergoes the photo-oxidation with relatively low-energy orange light ($\lambda_{ex} \approx 590$ nm, 2.10 eV). To put that into perspective, the theoretical ideal gap-energy for solar energy conversion is ~1.25 eV, or absorbance around 1130 nm, as defined by the Shockley-Queisser limit while many pristine semiconductors used in *photocatalysis*[*] (ZrO, TiO_2, WO_3, *etc.*) have optical gap energies between 2.5 – 4.0 eV and require UV (<400 nm) light to preform catalysis without sensitizers.[18,20,56,57] Utilizing such relatively mild conditions and low-energy for production of a commercially relevant compound is highly desirable, in particular for H_2O_2 production. As previously discussed, the conditions for catalysis via tellurorhodamines hold a tremendous advantage when compared to the current industry standard of anthraquinone derivatives, which require pressurized gasses, alkane solvents, precious metal catalysts, extensive heating at moderate temperatures, as well as liquid-liquid extraction and intensive reflux.[6]

[*]Photovoltaic semiconductors, e.g. Silicon (E_g = 1.1 eV), differ fundamentally from photocatalytic semiconductors both in purpose and desirable characteristics; this comparison is being made for the purpose of forming an intuitive energy-scale.

While we have shown in previous work that **mesi** oxidation produces one equivalent of H_2O_2 upon oxidation, little work has been done to evaluate farther.[11] Catalytic efficiencies and viability of the molecules have yet to be established in any concrete terms. Additionally, it is unclear what the total possible production of the catalytic cycle is with respect to electrochemical cycling. Observations made throughout experimentation, including the pH dependence of observed in Figure 7, elude to the possibility that tellurorhodamines may produce an additional equivalent of H_2O_2 when the dye is electrochemically or thermally reduced. The reactivity of **mesiO** and H_2O_2 species in solution have made evaluations of such properties problematic in terms of each species' auto-catalyzed reactions. However, strenuous water and O_2 control can be used to isolate the species from one another to better probe the conditions of H_2O_2 catalysis by oxidation *and* reduction of the tellurorhodamine chromophores.

It is essential that, if **mesi** is ever intended to be used as a catalyst, its reduction products are verified. Up to this point, it has been assumed that H_2O is the sole reduction product in **mesi** solutions, as it is the byproduct of substrate driven chemical reduction previously documented.[10–12] It has been shown that tellurorhodamine oxides can also be reduced thermally and electrochemically, by this

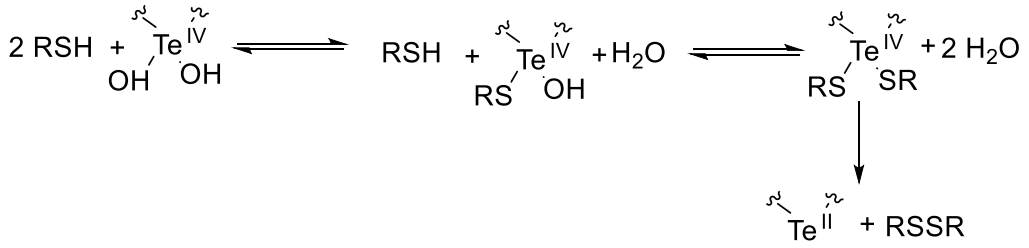

Scheme 4: Thiol oxidation pathway using mesi

and other work, and the difference in reduction pathway likely affects the expected products. In electrochemical and thermal reduction, the solution no longer has substrate to provide protons for balanced reduction as suggested in Scheme 4. It is possible that H_2O is the major product in the case of electrochemical reduction, but without an obvious, external source of electrons thermal reduction should only be able to proceed by one of two mechanisms. One possibility is that the reduction involved solvent breakdown. Given the redox stability of PC, oxidation of solvent for reduction of the catalyst seems unlikely, though possible. PC does undergo oxidation via a well-known pathway which may be compatible with **mesiO** reduction.[58–60] The mechanism would proceed as follows in Scheme 5:

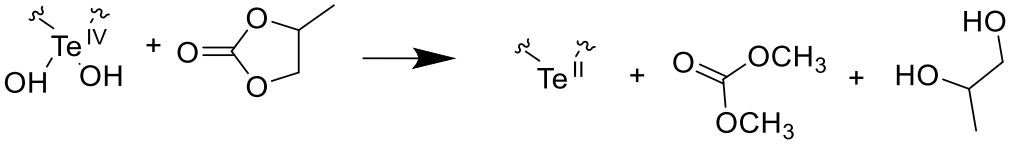

Scheme 5: Theoretical oxidation of propylene carbonate

The second possibility is reductive elimination:

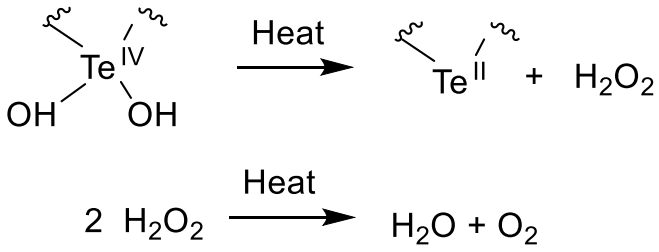

Scheme 6: Thermal reduction of mesiO and subsequent thermal decomposition of H_2O_2

In Scheme 6, the tellurium core of **mesiO** undergoes single electron exchanges with the coordinated hydroxyl groups, which in turn form a peroxide bond, generating H_2O_2. A similar mechanism is possible in electrochemical reduction, as it is well known that single-electron transfers happen more rapidly than 2-electron transfers, especially in chalcogen containing species which favor outer sphere

electron transfer.[50–52] Upon reduction of Te^{4+} to Te^{3+}, the more unstable oxidation state of tellurium, two separate molecules of **mesiO**$^-$ coordinate to generate 2 molcules of **mesi**, one molecule of H_2O_2, and 2 hydroxide ions (OH^-). The set of reactions could be represented as follows:

Chemical Reaction:

$$\mathbf{AryTe^{IV}(OH)_2 + 2HSR \rightarrow AryTe^{II} + 2H_2O + RSSR} \quad \textbf{, rxn 1}$$

Thiol Half-cell:

$$\mathbf{2HSR \rightarrow 2H^+ + RSSR + 2e^-} \quad \textbf{, rxn 2}$$

Mesi/O half-cell:

$$\mathbf{2AryTe^{IV}(OH)_2 + 2e^- \rightarrow [AryTe^{III}(OH)_2]^- + [AryTe^{III}(OH)_2]^-}$$

$$\mathbf{[\,Ary_2Te^{III}(OH)_2]^- + [Ary_2Te^{III}(OH)_2]^- \rightarrow 2Ary_2Te^{II} + H_2O_2 + 2OH^-}\textbf{, rxn 3}$$

Total Electrochemical Reaction:

$$\mathbf{2Ary_2Te^{IV}(OH)_2 + 2HSR \rightarrow 2Ary_2Te^{II} + 2H_2O + RSSR + H_2O_2} \quad \textbf{, rxn4}$$

Testing and verifying the reduction products of electrochemical and thermal reduction has proven difficult due to the presence of H_2O_2 in solution from **mesi** oxidation, but a method has been developed to address that difficulty. By maintaining temperature and potential within a sealed vessel past the point of visual reduction, any H_2O_2 which may have been produced upon reduction should be decomposed into water and O_2. In a system which has under gone rigorous air-exclusion, production of O_2 should be easily detected from gaseous mass analysis of the sample headspace. Within **mesiO** samples, if no H_2O_2 is produced and the products of reduction are simply water or bi-products of solvent breakdown, then no O_2 should be present in the sealed vessels. By separating **mesiO** from its parent solution by rapid-solvent evaporation, drying and reconstituting the crystals in

degassed solvent, there has been some success in isolating **mesiO** from H_2O_2, though partial reduction has been unavoidable.

4.2 Detection of H_2O_2

4.2.1 Titanium-Porphyrin Quantification of H_2O_2

One of the methods used previously to confirm production of H_2O_2 was first detailed by Matsubara *et al* in 1992.[47] They established an ultrasensitive technique for quantifying peroxi-compounds using Oxo [5, 10, 15, 20-tetra (4-pyridyl) porphyrinato] titanium(IV) (Ti-Pphy), and the quenching of its absorbance intensity as the porphyrin coordinates to and reacts with the peroxide

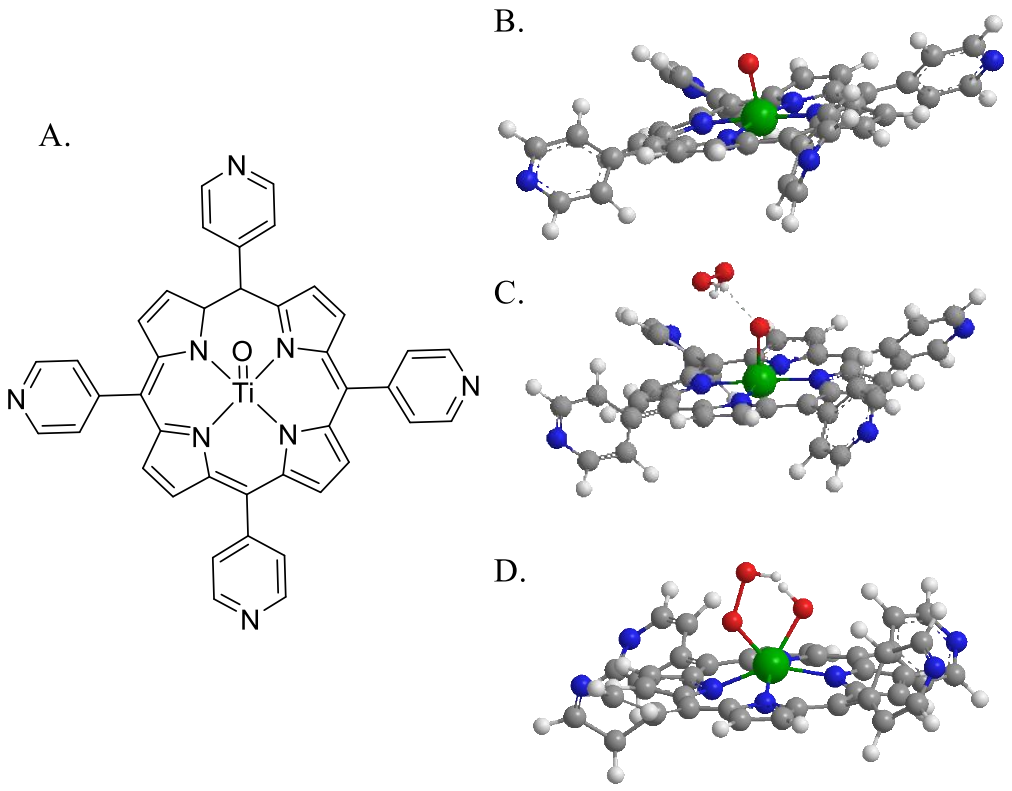

Figure 12: A and B) Stucture of Ti-Pphy; C) coordination of hydrogen peroxide to the oxygen of Ti-Pphy followed by D) coordination of super-oxide to the Ti core of Ti-Pphy which caused the change in absorbance observed in Figure 14

bond in molecules like H_2O_2 as seen in Figure 13. The coordination of H_2O_2 to the

oxygen and subsequent coordination and reaction of that H_2O_2 with the titanium core of Ti-Pphy, results in a shift in absorbance in the compound's UV-Vis spectrum sensitive enough to quantify H_2O_2 concentrations even in the nanomolar regime. In previous testing it was found that the presence of **mesi** does effect the absorbance profile of Ti-Pphy solutions, but it does not react with the porphyrin itself. However, **mesiO** was found to react 1:1 with the porphyrin, and so must be

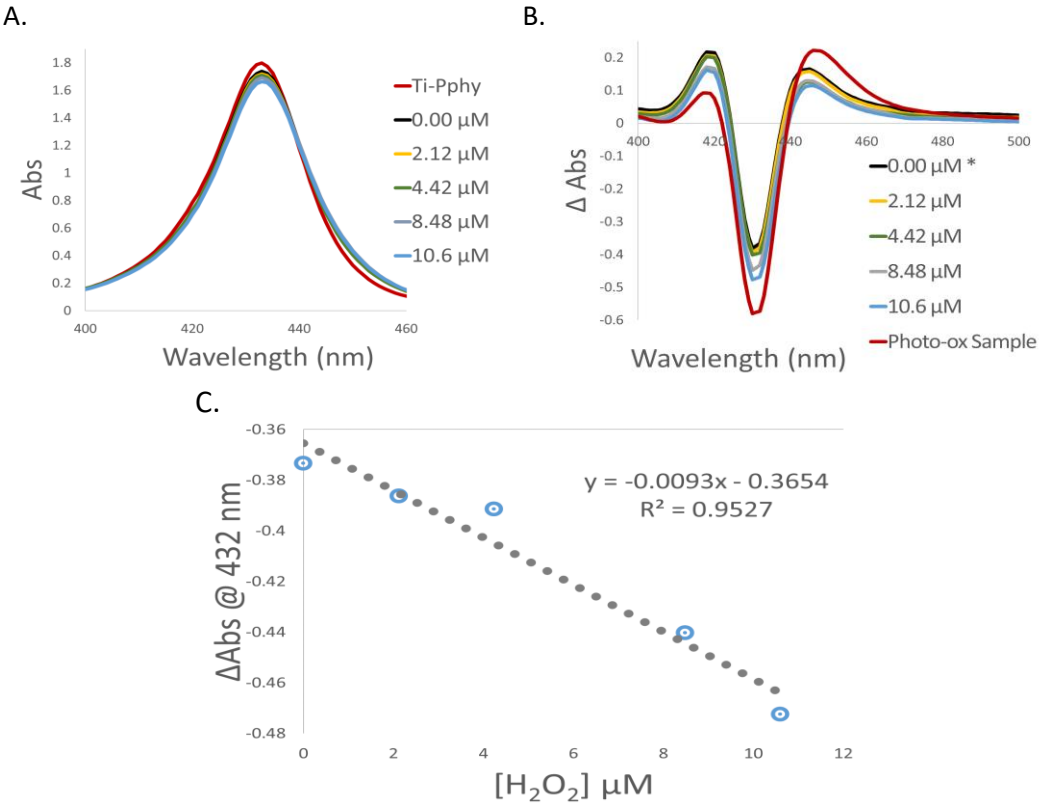

Figure 13: Standardization of Ti-Pphy response to hydrogen peroxide A) absolute absorbance around 432 nm peak B) spectra after subtraction of the initial Ti-Pphy spectrum, and C) calibrated to stock concentrations

accounted for in quantification. A sample solution of **mesiO** was prepared and read; the resulting spectrum can be seen in Figure 14. While at first glance the change in absorbance seems miniscule (Figure 14.A), once the initial Ti-Pphy spectral profile is removed from the subsequent traces (Figure 14.B), the pattern of absorbance peak suppression becomes much clearer. The resultant curve

achieves a respectable correlation for the concentration of peroxide even at micromolar concentrations.

4.2.2 Mass Analysis of Gaseous Mesi/O Reduction Products

According to Scheme 6, with careful air exclusion the headspace of sealed samples can be analyzed to help determine the reduction product of **mesiO**, or simply exclude H_2O_2. If Scheme 6 is accurate, or the set of electrochemical reactions in Section 4.1 in the case of electrochemical reduction, then H_2O_2 is being produced upon reduction of **mesiO** and decomposition of that H_2O_2 should yield O_2 in the headspace of sealed vessels. However, if water is the reduction product as suspected in the case of the chemical reduction in scheme 4, or the system uses solvent driven reduction, as seen in Scheme 5, then O_2 can be expected to be absent from sealed vessels post reduction. While not a perfect measure for the identification of a reduction product, this headspace analysis can provide key insight for development of methodology of the desired identification within the fickle **mesi/O** system.

Two isolated samples of **mesiO** were prepared in PC at 1.0 mM and split between sealed flasks and open vials. After being reduced, the samples were read by mass analysis of the headspace for O_2; results of the test can be seen in Figure 15. Definite spikes in O_2 concentration correlated to sample injection give a good, though not definite indication that H_2O_2 is being produced upon reduction of **mesiO.**

4.2.3 H_2O_2 Quantification Discussion & Results

It is safe to say that H_2O_2 is playing a key role in the chemical behavior of this system. Detection and quanitification of H_2O_2 has been made difficult by the inexerably linked chemical reactivity of the **mesi/O** solution, regardles of the chosen solvent system. While the presence of H_2O_2 can be confirmed after oxidation and after reduction, back-reaction and spontaneous decay continue to make *in-situ* quantification of H_2O_2 difficult.

The corresponding shift in absorbance observed in Figure 14.A&B indicated a total concentration shift of 7.44 µM Ti-Pphy. That shift of Ti-Pphy corresponds to an *in-situ* concentration of 22.3 µM, and when accounting for the **mesiO** in solution would indicate that the H_2O_2 concentration was 10.3 µM. As mentioned before, interactions between H_2O_2 and **mesiO** create complications in quantification, and so it's not unreasonable to assume some back reaction

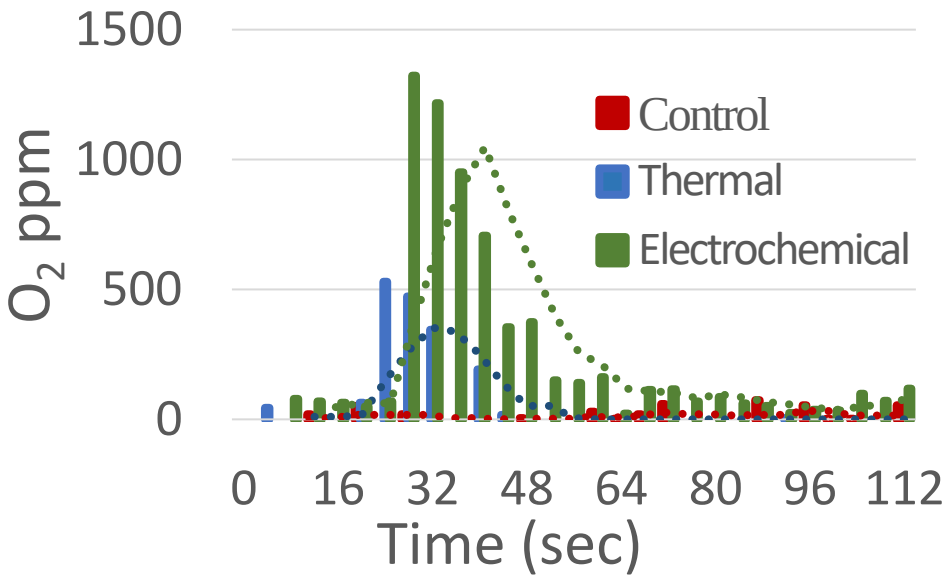

Figure 14: Headspace analysis for O_2 of isolated mesiO samples reduced back to mesi via electrochemical and thermal processes

accounting for the apparent 14% loss when compared to the expected 1:1 H_2O_2 generation at 12 µM **mesi**. Additional methods are being developed to minimize complications from back reaction for future experiments aimed at accumulation of H_2O_2, such as use of stabilizing agents like urea, and bi-phasic approaches for separation fo the two species. Iodide determination of H_2O_2 has proven to be very reliable, but in the presence of **mesi/O** shifts in absorbance peaks make the approach unusable for these reaction mixtures; the shift is thought to be from iodide coordination to the tellurium core of **mesi**.

Thermal and electrochemical reduction also suffered from issues of quantification, though they seemed to yield positive results in detection of H_2O_2. In Figure 16, it can be plainly seen that there are significant O_2 spikes which correspond to sample injection that are absent from the PC control. The difference in peak height between the thermal and electrochemical trace is thought to be due to the difference in preparation and processing between the samples. The change in pressure resulting from heating in the sealed vessel, despite precautions, likely led to O_2 and other gases leaking out of the RB-flask, whereas the electrochemical sample was not expected to experience the same degree of pressure change and to only produce half the volume of O_2, according to the proposed reaction, rxn 4. Even so, the significant presence of O_2 in both samples seems to indicate that the major product of reduction is not H_2O as was previously thought. Our current hypothesis is that H_2O_2 is being produced upon reduction as well as oxidation of the catalyst, but more testing is required to positively confirm that claim. It is possible that some mixture of O_2 and H_2O is being produced directly upon reduction,

though the greater complexity of a mechanism required for direct O_2 elimination makes that case seem unlikely.

5. Conclusion

Whether or not the use of H_2O_2 as a fuel source constitutes a long-term solution to growing global energy demands is a prospect which may ultimately never be explored with the current strides being made with other energy sources. In light of the current conflicts surrounding fossil fuels it stands to reason that a diversity of energy sources should be pursued regardless of the promise and/or application of any particular source. Given that the **mesi/O** system has already been shown to produce H_2O_2 in such favorable conditions compared to the industry standard, the results presented in this work seem to imply that H_2O_2 may be a more attainable fuel than it is currently considered to be. Thus further research and development of PFC's and H_2O_2 production will be essential to the future of energy technology, and tellurorhodamine chomophores are an excellent starting point for a small molecule approach to alternative energy.

The structure of the tellurorhodamines can be further developed or optimized for catalysis, but the **mesi/O** system even as it stands has electrochemical and photochemical properties which are favorable to catalysis. The possibility of a second equivalent of H_2O_2 upon electrochemical reductions makes it an even more desirable target, but even lacking that, the positive reduction potential associated with **mesiO** makes it possible to reduce the dye while also being able to produce a working current when paired with an appropriate half-cell. According to Figure 12 electrochemical reduction is the limiting process in the **mesi/O** half-cell, evidenced by plateauing of the charging phases, which is in contrast to the photolimited **mesi** resting state previously observed in chemical reduction.[11] This

indicates that it is likely that an electrochemical cell with the **mesi/O** half-cell would be able to continuously produce current in continued illumination with minimal intensity light and undergo a long, sustained discharge when light is unavailable. The generation of an electrochemical working-current and simultaneous production of the energy storage molecule H_2O_2 make the **mesi/O** system unique among photoelectrochemical cathodes, and a highly desirable target for alternative energy research. Future research for the system should focus on effective separation of H_2O_2 from the **mesi/O** system as its continued presence has complicated clear characterization of the system and will continue to be the fundamental blockade in practical applications of tellurorhodamines as catalysts.

6 References

(1) REN21. *Renewables 2014: Global Status Report*; REN21, 2014.

(2) DOE. DOE Hydrogen and Fuel Cells Program: Hydrogen Storage. *U.S Dep. Energy* **2009**, *25*, 6.

(3) Nayak, P. K.; Erickson, E. M.; Schipper, F.; Penki, T. R.; Munichandraiah, N.; Adelhelm, P.; Sclar, H.; Amalraj, F.; Markovsky, B.; Aurbach, D. Review on Challenges and Recent Advances in the Electrochemical Performance of High Capacity Li- and Mn-Rich Cathode Materials for Li-Ion Batteries. *Adv. Energy Mater.* **2018**, *8* (8), 1–16. https://doi.org/10.1002/aenm.201702397.

(4) Luo, N.; Miley, G. H.; Shrestha, P. J.; Gimlin, R.; Burton, R.; Rusek, J.; Holcomb, F. H2O2-Based Fuel Cells for Space Power Systems. *J. Propuls. Power* **2008**, *24* (3), 583–589.

(5) Kato, S.; Jung, J.; Suenobu, T.; Fukuzumi, S. Production of Hydrogen Peroxide as a Sustainable Solar Fuel from Water and Dioxygen. *Energy Environ. Sci.* **2013**, *6* (12), 3756. https://doi.org/10.1039/c3ee42815j.

(6) Campos-Martin, J. M.; Blanco-Brieva, G.; Fierro, J. L. G. Hydrogen Peroxide Synthesis: An Outlook beyond the Anthraquinone Process. *Angew. Chemie - Int. Ed.* **2006**, *45* (42), 6962–6984. https://doi.org/10.1002/anie.200503779.

(7) Fukuzumi, S. Artificial Photosynthesis for Production of Hydrogen Peroxide and Its Fuel Cells. *Biochim. Biophys. Acta* **2015**. https://doi.org/10.1016/j.bbabio.2015.08.012.

(8) Masuda, T.; Fujishima, M.; Tada, H. Photo-Effect on the Electromotive Force in Two-Compartment Hydrogen Peroxide-Photofuel Cell. *Electrochem. commun.* **2018**, *93* (June), 31–34. https://doi.org/10.1016/j.elecom.2018.05.025.

(9) Detty, M. R. Reaction Pathways of Telluroxide Equivalents. Reductive Elimination of Hydrogen Peroxide from Dihydroxytelluranes and Oxidation of Carbon via Intramolecular Transfer of Oxygen. *Organometallics* **1991**, *10* (3), 702–712.

(10) You, Y.; Ahsan, K.; Detty, M. R. Mechanistic Studies of the Tellurium (II)/ Tellurium (IV) Redox Cycle in Thiol Peroxidase-like Reactions of Diorganotellurides in Methanol. *J. Am. Chem. Soc.* **2003**, No. II, 4918–4927.

(11) Lutkus, L. V.; Irving, H. E.; Davies, K. S.; Hill, J. E.; Lohman, J. E.;

Eskew, M. W.; Detty, M. R.; McCormick, T. M. Photocatalytic Aerobic Thiol Oxidation with a Self-Sensitized Tellurorhodamine Chromophore. *Organometallics* **2017**, *36* (14), 2588–2596. https://doi.org/10.1021/acs.organomet.7b00166.

(12) Wadsworth, D. H.; Detty, M. R. Regiochemical Control of the Addition of Aryl Selenols and Aryl Thiols to the Triple Bond of Arylpropiolates. Synthesis of Seleno- and Thioflavones and Seleno- and Thioaurones. *J. Org. Chem.* **1980**, *45* (23), 4611–4615. https://doi.org/10.1021/jo01311a013.

(13) Detty, M. R.; Friedman, A. E.; Oseroff, A. R. A Mechanism for the Oxidation of Glutathione to Glutathione Disulfide with Organotellurium(IV) and Organoselenium(IV) Compounds. A Stepwise Process with Implications for Photodynamic Therapy and Other Oxidative Chemotherapy Michael. *J. Org. Chem.* **1994**, *59* (4), 8245–8250.

(14) Ni, M.; Leung, M. K. H.; Leung, D. Y. C.; Sumathy, K. A Review and Recent Developments in Photocatalytic Water-Splitting Using TiO2 for Hydrogen Production. *Renew. Sustain. Energy Rev.* **2007**, *11* (3), 401–425. https://doi.org/10.1016/j.rser.2005.01.009.

(15) Yamabi, S.; Imai, H. Crystal Phase Control for Titanium Dioxide Films by Direct Deposition in Aqueous Solutions. *Chem. Mater.* **2005**, *14* (20), 609–614.

(16) Peiró, A. M.; Vigil, E.; Peral, J.; Domingo, C.; Domènech, X.; Ayllón, J. A. Titanium(IV) Oxide Thin Films Obtained by a Two-Step Soft-Solution Method. *Thin Solid Films* **2002**, *411* (2), 185–191. https://doi.org/10.1016/S0040-6090(02)00276-6.

(17) Saba, M.; Aresti, M.; Quochi, F.; Marceddu, M.; Loi, M. A.; Huang, J.; Talapin, D. V; Mura, A.; Bongiovanni, G.; Al, S. E. T. Light-Induced Charged and Trap States in Colloidal Nanocrystals Detected by Variable Pulse Rate Photoluminescence Spectroscopy. **2013**, No. 1, 229–238.

(18) Sayama, K.; Arakawa, H. Photocatalytic Decomposition of Water and Photocatalytic Reduction of Carbon-Dioxide over Zro2 Catalyst. *J. Phys. Chem.* **1993**, *97*, 531–533. https://doi.org/10.1021/J100105a001.

(19) Margraf, J. T.; Ruland, A.; Sgobba, V.; Guldi, D. M.; Clark, T. Theoretical and Experimental Insights into the Surface Chemistry of Semiconductor Quantum Dots. *Langmuir* **2013**, *29* (49), 15450–15456. https://doi.org/10.1021/la403633e.

(20) Bard, A. J. Photoelectrochemistry and Heterogeneous Photo-Catalysis at Semiconductors. *J. Photochem.* **1979**, *10* (1), 59–75.

https://doi.org/10.1016/0047-2670(79)80037-4.

(21) Woodward, S. Homogeneous Catalysis by Transition Metal Complexes. *Organomet. Chem.* **2007**, *182*, 353–390. https://doi.org/10.1039/9781847554093-00353.

(22) Hong, D.; Tsukakoshi, Y.; Kotani, H.; Ishizuka, T.; Ohkubo, K.; Shiota, Y.; Yoshizawa, K.; Fukuzumi, S.; Kojima, T. Mechanistic Insights into Homogeneous Electrocatalytic and Photocatalytic Hydrogen Evolution Catalyzed by High-Spin Ni(II) Complexes with S2N2-Type Tetradentate Ligands. *Inorg. Chem.* **2018**, *57* (12), 7180–7190. https://doi.org/10.1021/acs.inorgchem.8b00881.

(23) Kim, D. hyo; Lee, D.; Monllor-Satoca, D.; Kim, K.; Lee, W.; Choi, W. Homogeneous Photocatalytic Fe3+/Fe2+ Redox Cycle for Simultaneous Cr(VI) Reduction and Organic Pollutant Oxidation: Roles of Hydroxyl Radical and Degradation Intermediates. *J. Hazard. Mater.* **2018**, No. November 2017, 0–1. https://doi.org/10.1016/j.jhazmat.2018.03.055.

(24) Fukuzumi, S.; Jung, J.; Yamada, Y.; Kojima, T.; Nam, W. Homogeneous and Heterogeneous Photocatalytic Water Oxidation by Persulfate. *Chem. - An Asian J.* **2016**, *11* (8), 1138–1150. https://doi.org/10.1002/asia.201501329.

(25) Zhang, G.; Lan, Z. A.; Wang, X. Merging Surface Organometallic Chemistry with Graphitic Carbon Nitride Photocatalysis for CO2 Photofixation. *ChemCatChem* **2015**, *7* (9), 1422–1423. https://doi.org/10.1002/cctc.201500133.

(26) Grätzel, M. Dye-Sensitized Solar Cells. *J. Photochem. Photobiol. C Photochem. Rev.* **2003**, *4* (2), 145–153. https://doi.org/10.1016/S1389-5567(03)00026-1.

(27) Gong, J.; Sumathy, K.; Qiao, Q.; Zhou, Z. Review on Dye-Sensitized Solar Cells (DSSCs): Advanced Techniques and Research Trends. *Renew. Sustain. Energy Rev.* **2017**, *68* (September 2016), 234–246. https://doi.org/10.1016/j.rser.2016.09.097.

(28) Usami, a. Theoretical Simulations of Optical Confinement in Dye-Sensitized Nanocrystalline Solar Cells. *Sol. Energy Mater. Sol. Cells* **2000**, *64* (1), 73–83. https://doi.org/10.1016/S0927-0248(00)00049-0.

(29) Yu, M. H.; Yang, C. L.; Huang, Y. C.; Hsieh, I. C. A Fast Dye Sucking Method for Dye-Sensitized Solar Cell Fabrication. *Conf. Rec. IEEE Photovolt. Spec. Conf.* **2013**, *2*, 2761–2763. https://doi.org/10.1109/PVSC.2013.6745045.

(30) Karamshuk, S.; Caramori, S.; Manfredi, N.; Salamone, M.; Ruffo, R.; Carli, S.; Bignozzi, C. A.; Abbotto, A. Molecular Level Factors Affecting the Efficiency of Organic Chromophores for P-Type Dye Sensitized Solar Cells. *Energies* **2016**, *9* (1). https://doi.org/10.3390/en9010033.

(31) Graetzel, M. Photoelectrochemical Cells; Review. *Nature* **2001**, *414* (9518), 338–344. https://doi.org/10.1016/S0140-6736(06)68542-5.

(32) Khaselev, O.; Turner, J. A. A Monolithic Photovoltaic-Photoelectrochemical Device for Hydrogen Production via Water Splitting.

(33) Arango, A. C.; Oertel, D. C.; Xu, Y.; Bawendi, M. G.; Bulovic, V. Heterojunction Photovoltaics Using Printed Colloidal Quantum Dots as a Photosensitive Layer. *Nano Lett.* **2009**, *9*, 860–863. https://doi.org/10.1021/n1803760j.

(34) Hou, Y.; Qiu, M.; Zhang, T.; Ma, J.; Liu, S.; Zhuang, X.; Yuan, C. Efficient Electrochemical and Photoelectrochemical Water Splitting by a 3D Nanostructured Carbon Supported on Flexible Exfoliated Graphene Foil. **2016**, 1–7. https://doi.org/10.1002/adma.201604480.

(35) Scanlon, M. D.; Peljo, P.; Rivier, L.; Vrubel, H.; Girault, H. H. Mediated Water Electrolysis in Biphasic Systems. *Phys. Chem. Chem. Phys.* **2017**, *19* (34), 22700–22710. https://doi.org/10.1039/c7cp04601d.

(36) Makridis. Hydrogen Storage and Compression. *Methane Hydrog. Energy Storage* **2016**, No. June, 1–28. https://doi.org/10.1049/PBPO101E_ch1.

(37) Liu, C.; Ziesack, M.; Silver, P. A. Water Splitting – Biosynthetic System with CO 2 Reduction Efficiencies Exceeding Photosynthesis. *Science (80-.).* **2016**, *352* (6290), 1210–1213.

(38) Wang, M.; Han, K.; Zhang, S.; Sun, L. Integration of Organometallic Complexes with Semiconductors and Other Nanomaterials for Photocatalytic H2 Production. *Coord. Chem. Rev.* **2015**, *287*, 1–14. https://doi.org/10.1016/j.ccr.2014.12.005.

(39) Hou, Y.; Qiu, M.; Zhang, T.; Ma, J.; Liu, S.; Zhuang, X.; Yuan, C. Efficient Electrochemical and Photoelectrochemical Water Splitting by a 3D Nanostructured Carbon Supported on Flexible Exfoliated Graphene Foil. *Adv. Mater.* **2016**, 1–7. https://doi.org/10.1002/adma.201604480.

(40) Adachi, K.; Ohta, K.; Mizuno, T. Photocatalytic Reduction of Carbon Dioxide to Hydrocarbon Using Copper-Loaded Titanium Dioxide. *Sol. energy* **1994**, *53* (2), 187–190. https://doi.org/10.1016/0038-092X(94)90480-4.

(41) Ishitani, O.; Inoue, C.; Suzuki, Y.; Ibusuki, T.; Ishitani|, O.; Inoue, C.; Suzuki, Y.; Ibusuki, T. Photocatalytic Reduction of Carbon Dioxide to Methane and Acetic Acid by an Aqueous Suspension of Metal-Deposited TiO 2. *J. Photochem. …* **1993**, *72* (3), 269–271. https://doi.org/10.1016/1010-6030(93)80023-3.

(42) Tan, S. S.; Zou, L.; Hu, E. Photocatalytic Reduction of Carbon Dioxide into Gaseous Hydrocarbon Using TiO2 Pellets. *Catal. Today* **2006**, *115* (1–4), 269–273. https://doi.org/10.1016/j.cattod.2006.02.057.

(43) Wu, G.; Swaidan, R.; Cui, G. Electrooxidations of Ethanol, Acetaldehyde and Acetic Acid Using PtRuSn/C Catalysts Prepared by Modified Alcohol-Reduction Process. *J. Power Sources* **2007**, *172* (1), 180–188. https://doi.org/10.1016/j.jpowsour.2007.07.034.

(44) Shanmugam, S.; Xu, J.; Boyer, C. Photoinduced Oxygen Reduction for Dark Polymerization. *Macromolecules* **2017**, *50* (5), 1832–1846. https://doi.org/10.1021/acs.macromol.7b00192.

(45) Del Valle, D. J.; Donnelly, D. J.; Holt, J. J.; Detty, M. R. 2,7-Bis-N,N-Dimethylaminochalcogenoxanthen-9-Ones via Electrophilic Cyclization with Phosphorus Oxychloride. *Organometallics* **2005**, *24* (15), 3807–3810. https://doi.org/10.1021/om050225o.

(46) Inamo, M.; Funahashi, S.; Tanaka, M. Kinetics of the Reaction of Hydrogen Peroxide with Some Oxotitanium(IV) Complexes as Studied by a High-Pressure Stopped-Flow Technique1. *Inorg. Chem.* **1983**, *22* (25), 3734–3737. https://doi.org/10.1021/ic00167a013.

(47) Matsubara, C.; Kawamoto, N.; Takamura, K. Oxo[5, 10, 15, 20-Tetra(4-Pyridyl)Porphyrinato]Titanium(IV): An Ultra-High Sensitivity Spectrophotometric Reagent for Hydrogen Peroxide. *Analyst* **1992**, *117* (11), 1781. https://doi.org/10.1039/an9921701781.

(48) Luther, G. W.; Findlay, A. J.; MacDonald, D. J.; Owings, S. M.; Hanson, T. E.; Beinart, R. A.; Girguis, P. R. Thermodynamics and Kinetics of Sulfide Oxidation by Oxygen: A Look at Inorganically Controlled Reactions and Biologically Mediated Processes in the Environment. *Front. Microbiol.* **2011**, *2* (APR), 1–9. https://doi.org/10.3389/fmicb.2011.00062.

(49) Luo, D.; Smith, S. W.; Anderson, B. D. Kinetics and Mechanism of the Reaction of Cysteine and Hydrogen Peroxide in Aqueous Solution. *J. Pharm. Sci.* **2005**, *94* (2), 304–316. https://doi.org/10.1002/jps.20253.

(50) Freedman, Leon D (Chemical Laboratory of the Johns Hopkins University, B.; MD); Corwin, A. H. Oxidation-Reduction Potentials of Thiol-Disulfide Systems. *J. Biol. Chem.* **1949**, No. 181, 601–621.

(51) Randall, L. O. REACTION OF THIOL COMPOUNDS WITH PEROXIDASE AND HYDROGEN PEROXIDE. *J. Biol. Chem.* **1946**, *164*, 521–527.

(52) Stein, C. A.; Taube, H. Manifestations of Sulfur to Sulfur Through-Space Interactions in Complex Ion Spectra. *J. Am. Chem. Soc.* **1978**, *100* (6), 1635–1637. https://doi.org/10.1039/c8cc07949h.

(53) Nadezhdin, A. D.; Dunford, H. B. The Oxidation of Ascorbic Acid and Hydroquinone by Perhydroxyl Radicals. A Flash Photolysis Study. *Can. J. Chem.* **1979**, *57* (12), 3017–3022.

(54) Cofré, P.; Sawyer, D. T. Electrochemical Reduction of Dioxygen to Perhydroxyl (HO2 ·) in Aprotic Solvents That Contain Brønsted Acids. *Anal. Chem.* **1986**, *58* (6), 1057–1062. https://doi.org/10.1021/ac00297a017.

(55) Baba, Y.; Yatagai, T.; Harada, T.; Kawase, Y. Hydroxyl Radical Generation in the Photo-Fenton Process: Effects of Carboxylic Acids on Iron Redox Cycling. *Chem. Eng. J.* **2015**, *277*, 229–241. https://doi.org/10.1016/j.cej.2015.04.103.

(56) Tang, J.; Durrant, J. R.; Klug, D. R. Mechanism of Photocatalytic Water Splitting in TiO_2. Reaction of Water with Photoholes, Importance of Charge Carrier Dynamics, and Evidence for Four-Hole Chemistry. *J. Am. Chem. Soc.* **2008**, *130* (42), 13885–13891. https://doi.org/10.1021/ja8034637.

(57) Morra, E.; Giamello, E.; Chiesa, M. EPR Approaches to Heterogeneous Catalysis. The Chemistry of Titanium in Heterogeneous Catalysts and Photocatalysts. *J. Magn. Reson.* **2017**, *280*, 89–102. https://doi.org/10.1016/j.jmr.2017.02.008.

(58) Arakawa, M.; Yamaki, J. ichi. Anodic Oxidation of Propylene Carbonate and Ethylene Carbonate on Graphite Electrodes. *J. Power Sources* **1995**, *54* (2), 250–254. https://doi.org/10.1016/0378-7753(94)02078-H.

(59) Atanasoski, R. T.; Law, H. H.; McIntosh, R. C.; Tobias, C. W. Electrochemical Analysis of Trace Amounts of Water in Propylene Carbonate Electrolytes. *Electrochim. Acta* **1987**, *32* (6), 877–886. https://doi.org/10.1016/0013-4686(87)87077-9.

(60) Leggesse, E. G.; Lin, R. T.; Teng, T. F.; Chen, C. L.; Jiang, J. C. Oxidative Decomposition of Propylene Carbonate in Lithium Ion Batteries: A DFT Study. *J. Phys. Chem. A* **2013**, *117* (33), 7959–7969. https://doi.org/10.1021/jp403436u.